

LANGUAGE MAPPING WITH DENSE ARRAY EEG SOURCE LOCALIZATION:  
IMPLICATIONS FOR NEUROSURGICAL PLANNING

by

JOSEPH MICHAEL NELSON

A THESIS

Presented to the Department of Psychology  
and the Graduate School of the University of Oregon  
in partial fulfillment of the requirements  
for the degree of  
Master of Science

June 2012

THESIS APPROVAL PAGE

Student: Joseph Michael Nelson

Title: Language Mapping with Dense Array EEG Source Localization: Implications for Neurosurgical Planning

This thesis has been accepted and approved in partial fulfillment of the requirements for the Master of Science degree in the Department of Psychology by:

Don Tucker	Chairperson
Catherine Poulsen	Member
Dare Baldwin	Member

and

Kimberly Andrews Espy	Vice President for Research & Innovation/Dean of the Graduate School
-----------------------	--

Original approval signatures are on file with the University of Oregon Graduate School.

Degree awarded June 2012

© 2012 Joseph Michael Nelson

## THESIS ABSTRACT

Joseph Michael Nelson

Master of Science

Department of Psychology

June 2012

Title: Language Mapping with Dense Array EEG Source Localization: Implications for Neurosurgical Planning

Current language mapping protocols for neurosurgical planning are invasive, expensive, and not suitable for all surgical candidates. We investigated the potential of dense array EEG to determine hemispheric dominance for language and localize current sources of semantic and lower level language functions in the brain using a semantic decision task, a phonological decision task, and an acoustic decision task. Source estimates of N400-window ERPs (N365, N480) and the Late Positive Complex (LPC) localized strongly to medial temporal regions. Overall source estimates revealed a slight left lateralized network, with more posterior engagement for the semantic condition and more anterior engagement for the phonological condition. Source localization of the resulting t-test wave from the semantic – phonological highlighted a stronger left lateralized pattern of activation encompassing more of the semantic network. As a first pass these results are promising, but need to be investigated on individual subject ERPs.

## CURRICULUM VITAE

NAME OF AUTHOR: Joseph Michael Nelson

GRADUATE AND UNDERGRADUATE SCHOOLS ATTENDED:

University of Oregon, Eugene  
Rogue Community College, Grants Pass, Oregon

DEGREES AWARDED:

Master of Science, Psychology, University of Oregon, 2012  
Bachelor of Science, Psychology, University of Oregon, 2010  
Associate of Arts, Oregon Transfer, Rogue Community College, 2007

AREAS OF SPECIAL INTEREST:

Cognitive Neuroscience  
Electrophysiology  
Language

PROFESSIONAL EXPERIENCE:

Research Assistant, Electrical Geodesics Inc., 4 years

## PUBLICATIONS:

Poulsen, C., Luu, P., Davey, C., Tucker, D., & **Nelson, J.** (2011). From sound to meaning: changes in EEG source-localized brain activity with foreign-language training. In D.D. Schmorrow and C.M. Fidopiastis (Eds.): FAC 2011, HCII 2011, LNAI 6780, pp. 203–211. Springer-Verlag: Berlin.

## ACKNOWLEDGMENTS

I wish to express sincere appreciation to my committee member Catherine Poulsen for her enthusiasm, critical guidance, and availability in the preparation of this manuscript. Also, special thanks to the science team at Electrical Geodesics Inc., my advisor Don Tucker and Phan Luu, for their guidance in this research. I also want to thank my committee member Dare Baldwin for helping to keep me on track and always having her door open. Of course thanks to thank my lab mates Alison Waters and Ida Moab for their support and wisdom, and the research assistant team in the brain electrophysiology lab, namely Jenn Lewis, Christopher Tompkins, Ally Davis, Stephanie Berger, and Mackenzie Keller for their assistance in participant scheduling and stimulus preparation. In addition, special thanks are due to my family Jim Nelson, Tracie Nelson, and Jimmy Nelson for all their support and encouragement.

# TABLE OF CONTENTS

Chapter	Page
I. INTRODUCTION.....	1
Overview.....	1
Language Organization.....	2
Task Considerations.....	3
Direct Cortical Stimulation.....	4
Functional Magnetic Resonance Imaging.....	4
Dense Array Electroencephalography.....	6
Electrophysiological Indices of Speech Processing.....	7
Hypotheses.....	8
II. METHODS.....	9
Participants.....	9
Materials and Apparatus.....	10
Stimuli.....	10
Tone Trains.....	10
Word Stimuli.....	11
Consonant-Vowel (CV) Triplets.....	12
Procedure.....	13
Design.....	15



Chapter	Page
Rationale and Independent Variables .....	15
EEG Recording and Preprocessing.....	15
Measures .....	16
Contrasts.....	18
Source Estimates .....	18
III. RESULTS .....	20
Event-Related Potentials (ERPs) .....	20
P1-N1-P2 Complex .....	20
P1 Latency Window (34—78ms) .....	20
N1 Latency Window (80—156ms) .....	24
P2 Latency Window (148—280ms) .....	24
N400-Window Components .....	26
N365 Latency Window (285—382ms) .....	26
N480 Latency Window (416—546ms) .....	27
P365 Latency Window (285—382ms) .....	28
Late Components .....	29
Late Positive Complex Latency Window (600—900ms) .....	29
Late Anterior Ventral Positivity (LAVP) Latency Window (642—950ms) .....	30
Late Frontal Negativity (LFN) Latency Window (550—1100ms) .....	30
Source Localization .....	34

Chapter	Page
Source Waveforms.....	34
N400-Window Components .....	34
N365/P365 .....	34
N480.....	34
Late Components .....	36
LPC 650ms.....	36
LAVP .....	38
LPC 850ms.....	39
Difference Wave Source Analysis vs. fMRI Subtraction .....	40
IV. DISCUSSION.....	42
Early Components.....	42
N400-Window Components .....	43
Scalp.....	43
N400-Window Source Localization .....	46
Later Components.....	47
LPC—Consistent With P3b .....	47
Late Component Source Localization .....	48
LAVP .....	49
Semantic – Phoneme T-test Wave .....	50
Limitations .....	51
Conclusions.....	52

APPENDICES .....	53
A. EDINBURGH HANDEDNESS INVENTORY .....	53
B. BLOCK DESIGN COUNTERBALANCING .....	54
C. SEMANTIC CONDITION STIMULUS LIST .....	55
D. PHONOLOGICAL CONDITION STIMULUS LIST.....	56
E. ACOUSTIC CONDITION STIMULUS LIST .....	57
REFERENCES CITED.....	58

## LIST OF FIGURES

Figure	Page
1. Trial Design .....	14
2. ERP Electrode Groupings.....	21
3. Grand Average ERPs .....	22
4. P1-N1-P2 Complex Waveforms.....	25
5. P1-N1-P2 Complex Topographical Maps.....	27
6. N400-Window and Later Component Topographic Maps .....	31
7. ERPs at Posterior Scalp Locations.....	32
8. ERPs at Anterior Scalp Locations.....	33
9. Source Waveforms.....	35
10. Source Solution at 365 ms (Approximate Peak of the N365) for Phonological and Semantic Grand Average ERPs .....	36
11. Source Solution at 480 ms (approximate peak of the N480) for Phonological and Semantic Grand Average ERPs. ....	37

Figure	Page
12. Source Solution at 650 ms (Approximate Atart of the LPC) for Phonological and Semantic Grand Average ERPs .....	38
13. Source Solution at 750 Ms (Approximate Peak of the LAVP for Phonological and Semantic Grand Average ERPs .....	39
14. Source Solution at 850 Ms (Approximate Peak of the LPC) for Phonological and Semantic Grand Average ERPs .....	40
15. Topographic Maps of the Semantic – the Phonological Condition from 50 ms to 900 ms .....	44
16. MRI View Comparison With the Binder et al. (2008) Semantic - Phoneme Decision Tasks .....	45

## LIST OF TABLES

Table	Page
1. CV Triplet Structure Sets.....	12
2. Mean Amplitudes ( $\mu\text{V}$ ) and Standard Deviations for All ERPs at All Measured Electrode Sites .....	23

## CHAPTER I

### INTRODUCTION

#### **Overview**

In recent years neuroimaging methods have been used to map critical language areas for pre-surgical planning. Prior to recent advances in determining language lateralization (hemispheric dominance) across neuroimaging methods such as positron emission tomography (PET), functional magnetic resonance imaging (fMRI), magnetoencephalography (MEG), electroencephalography (EEG), and near-infrared spectroscopy (NIRS), the WADA test had been exclusively used for determining lateralization of critical language and memory functions. The WADA test was named after Canadian neurologist, Juhn Atsushi Wada who first described the procedure over 60 years ago (Wada, 1949). This procedure is now more commonly referred to as the intracarotid sodium amobarbital procedure (ISAP) or as the intracarotid amobarbital test (IAT). The IAT is considered to be the gold standard to which new methods for lateralizing language and memory function are compared (Baxendale, 2009). Still, the IAT is very invasive and carries risks far greater than alternative neuroimaging methods. The IAT involves anesthetizing each hemisphere of the brain separately and measuring language functioning of the opposite hemisphere. This is accomplished by placing a catheter in the femoral artery and navigating to the carotid arteries where a barbiturate is injected. Risks associated with this procedure include pain, bleeding, infection, and stroke. The ability to localize brain regions involved in language processing is another advantage that neuroimaging methods have over the IAT. Localizing intrahemispheric

brain regions pre-operatively can not only help guide the surgery but can also inform the decision to proceed with the surgery (in the case that the outcome of the surgery is likely to be less desirable than the patient's current state).

This study will use dense array EEG and linear-inverse source localization techniques to localize language function within a semantic decision paradigm adapted from the Binder, Swanson, Hammeke, & Sabsevitz (2008) fMRI study while examining known ERP components associated with language processing. Dense array EEG has some advantages over other neuroimaging methods, but also has its own unique challenges. As a first step the present study will not be looking at ERPs at the individual level but instead at the grand average level and comparing the lateralization and localization results to general language processing anatomy models and the Binder et al., 2008 fMRI grand average. A future step, and for presurgical planning purposes, would be to conduct this at the individual level with both dense array EEG source localization and validated language mapping methods.

### **Language Organization**

Language organization is far more complex than suggested by previous models of Broca's and Wernicke's areas. Recent language models based on lesion and neuroimaging data show complex and distributed networks involved in various aspects of language processing such as acoustics, phonology, semantics, orthography, syntax, and lexico-semantics. Hickok and Poeppel (2007) posit a dual stream model for language processing in which the ventral stream is involved in speech processing for comprehension, and the dorsal stream is involved in forming articulatory representations from acoustic speech signals. The dorsal stream is largely left dominant including



structures in the posterior frontal lobe and inferior parietal lobe, whereas the ventral stream is more bilaterally organized including structures from the middle and superior temporal lobes (Hickok & Poeppel, 2007). A review on the anatomy of language as measured by 100 fMRI studies also indicates involvement of several temporal, frontal, and inferior parietal regions for language processing, showing more complex processes involving brain regions further away from primary auditory cortex and more left lateralized. However, direct cortical stimulation studies (e.g. Ojemann, Ojemann, Lettich, & Berger, 1989) highlight a high amount of variability across individuals in the localization of cortical brain regions involved in language processing.

### **Task Considerations**

Because the organization of language is so complex and variable across individuals, it is essential to carefully consider the experimental and control tasks when designing a language mapping protocol. In fMRI there is typically an active task from which a contrast task is subtracted. This same principle is routinely applied to some EEG studies. The resulting wave is referred to as a difference wave. The idea is to maximize activations associated with the target function (e.g. language) and minimize activations not associated with that function. This is particularly important in the context of pre-surgical planning when the goal is to accurately identify and avoid resecting the eloquent cortex. If a task fails to identify eloquent cortex (i.e., cortex that if removed will result in loss of sensory processing or linguistic ability), these important cortical regions may be at risk for resection. Conversely, if a task identifies areas which are not eloquent cortices the craniotomy may be larger than necessary and prolong open brain exposure during direct cortical stimulation mapping.

## **Direct Cortical Stimulation**

Direct Cortical Stimulation (DCS) follows pre-surgical mapping and is the gold standard for intraoperative language mapping. DCS is electrical current applied to the exposed brain (with skull removed) and interrupts processing in the applied area. While stimulation is occurring, language function can be assessed. A variety of tasks are used to assess language function including counting (Lurito, 2000), sentence recitation (Yetkin, 1997), object naming (Roux, 2003), speech comprehension, reading (Tomczak, 2000), and verb generation (Bizzi, 2008). When a patient fails to perform effectively during stimulation, the stimulated area will be flagged as a critical language area.

## **Functional Magnetic Resonance Imaging**

fMRI has received the most attention in recent years in research and clinical applications for determining both lateralization of language and localization of intrahemispheric language regions preoperatively. As in DCS, fMRI task protocols vary considerably. Many use visual stimuli and some use auditory stimuli. Lateralization indices are calculated using different regions of interest across studies (that is some studies only consider voxel activations in a subset of the brain matter which are believed to be of particular interest); some use the whole brain, some use only frontal or temporal, and some use a mix of Brodmann areas. fMRI studies also vary in contrast conditions, significance thresholds, and interpretation of blood oxygen level dependent (BOLD) response. All of these factors can have a substantial impact on surgeon's decisions regarding the lateralization and localization of language functioning. Nevertheless, reviews of the fMRI literature for language localization (e.g. Swanson, Sabsevitz,

Hammeke, & Binder, 2007; Bookheimer, 2007) highlight a fair amount of consistency in localization of these language networks across studies, typically showing a left lateralized network for higher level language processing. While several showed concordance rates with IAT as high as 100% (e.g. Binder et al., 1996; Spreer et al., 2002) (specifically semantic paradigms), some studies showed lower concordance with IAT, one as low as 55% (Worthington et al., 1997).

A review of nine fMRI language mapping studies directly comparing their results to direct cortical stimulation indicated that while fMRI seems to be a helpful preoperative planning tool, it is not ready to replace DCS. Sensitivity measures ranged from 59% to 100% and specificity measures ranged from 0 to 97% (Giussani et al., 2010), where specificity refers to the measure brain regions important for language function that are correctly identified as such, and sensitivity refers to measure of brain regions not essential for language functioning that are correctly identified as such. fMRI also has a number of limitations. It measures the brain's hemodynamic response related to neural activity and is, therefore, an indirect measure of brain activity. Brain tumors and arteriovenous malformations can sometimes further complicate the interpretation of the BOLD response due to abnormal blood flow in the brain. Finally, some individuals are not suitable for an MRI scan, such as those with metal in their body (e.g. pacemakers, head plates), old tattoos, and claustrophobia.

The present study sought to employ an EEG paradigm adapted from the Binder et al. (2008) fMRI study for several reasons: 1) it used an active semantic task as the primary activation condition; 2) it used both active phoneme and tone contrasts which allowed for control over arousal, decision making, and lower level speech processes (i.e.

acoustic and phonological processing); 3) it was found to be 100% concordant with the IAT test (N=22); and 4) it was more ecologically valid because it used naturalistic auditory stimuli. Using active conditions is important because it requires participant to attend to a particular aspect of the stimuli which can enhance activity in brain regions associated with that processing. It is particularly important to also have active contrast conditions because if passive, participants minds can wander, accessing conceptual knowledge and processing word meanings which would lead to lower specificity of brain regions involved in language processing (Binder et al., 1999). The active contrasts also help to control for non-linguistic function such as attention, working memory, and decision making processes. The Binder et al., 2008 study used a semantic decision, phoneme decision, and tone decision task in order to conduct two contrasts: 1) semantic – phoneme which was thought to control for acoustic and phonological processing and leave only brain activations associated with semantic processing; 2) semantic – tone which was thought to control only for acoustic processing and leave activations for both semantic and phonological processing. The latter contrast was found to be 100% concordant with the IAT (Binder, 1995).

### **Dense Array Electroencephalography**

Dense array EEG may be yet another helpful tool for mapping language. Source localization with EEG has already shown to be valuable in localizing epileptic spikes at the individual level. For example, Holmes and colleagues (2010) found that dense array EEG source localization was concordant with intracranial monitoring of spikes in eight out of ten cases. However, localization of language functioning using dense array EEG presents new challenges for EEG source localization due to the complex and distributed

network for language processing there are likely to be many cortical regions active at the same and different times, which will make source localization and comparability with other neuroimaging methods difficult. EEG has millisecond precision whereas fMRI has a temporal resolution of about 1 second and is in many cases collapsed across several seconds. A unique source solution is generated for each millisecond, which makes the picture substantially more complex. Although seemingly cumbersome, this millisecond precision can be seen as an advantage, allowing for the assessment of the time course of cortical generators of EEG instead of just a single picture collapsed across several seconds of language processing as in fMRI (Michel et al., 2004). Additional advantages of EEG are that EEG is more affordable, is a direct measure of brain activity, and is more suitable for claustrophobic individuals.

### **Electrophysiological Indices of Speech Processing**

In the literature regarding auditory evoked potentials (AEPs) the P1, N1, and P2 have long been identified as cortical brain responses thought to reflect attending to and initial processing of spectral information (e.g. Hillyard, Hink, Schwent, & Picton, 1973). These components together can be referred to as the P1-N1-P2 complex. A later negative-going potential, the N400, peaks around 400 ms after the onset of a meaningful word or word-like stimulus in either visual or auditory domains. The N400 is often thought to index lexical-semantic access to stored representations (see Kutas & Federmeier, 2009 for a review).

EEG source localization suggests possible generators for the N400 in superior/middle temporal gyrus, inferior parietal lobe, and medial temporal lobe (Frishkoff, Tucker, Davey, & Scherg, 2004). MEG and event-related optical signal

(EROS) have also suggested these same sources (Helenius, Salmelin, Service, & Connolly, 1999; Halgren, et al., 2002; Tse, et al., 2007). A review by Lau, Phillips, and Poeppel (2008) used evidence from nine fMRI studies using a typical N400 semantic priming paradigm to try to better understand the localization of N400 generators. They found spurious activity in inferior frontal gyrus, inferior temporal gyrus and superior temporal gyrus, but highly consistent activations in the middle temporal gyrus.

### **Hypotheses**

Based on the previous literature, we hypothesize that participants will show the typical auditory P1-N1-P2 complex for the acoustic, phonological, and semantic conditions. For the semantic condition vs. phonological condition, we would expect to see an N400-like effect with the semantic condition having a larger negativity between 300 and 500 ms post-stimulus than the phonological condition. We also hypothesize that EEG source analysis of the grand average will reveal a primarily left lateralized network of brain regions. We expect to see this pattern for both the phonological and semantic conditions, and furthermore for the semantic – phonological difference (t-wave) topographies. Because the experimental conditions and proposed contrast were very carefully adapted from the Binder et al. (2008) fMRI study and only modified when necessary, we expect to see many similarities in active brain regions between these two studies.

## CHAPTER II

### METHODS

#### **Participants**

A total of 30 participants were recruited from the University of Oregon and from the Telemedicine & Advanced Technology Research Center (TATRC) database at Electrical Geodesics Inc. (EGI). The TATRC database consists of individuals in Lane County with an ethnic distribution representative of Lane County, who agreed to be contacted about future EEG studies. Of the 30 participants, 6 were discarded due to excessive EEG artifacts. Of the 24 remaining participants, 13 identified as female and 11 identified as male. All participants identified as right handed (with a mean of 77 on the Edinburgh Handedness Inventory) between ages 19 and 64 years (mean of 26) with English as their primary language. Participants indicated no history of head trauma, psychological, neurological, or auditory disorders, and were not taking any drugs that would affect their EEG.

All participants gave informed consent prior to participation and received \$30 in remuneration. The study was approved by the institutional review boards at Electrical Geodesics Inc., and the University of Oregon.

## **Materials and Apparatus**

### **Stimuli**

There were three different types of auditory stimuli: a sequence of three tones (tone trains), a sequence of three consonant-vowel pairs (CV triplets), and three-syllable English words (word stimuli). The 3 stimulus types corresponded to the three experimental conditions: acoustic (tone trains), phonological (CV triplets), and semantic (word stimuli). All stimuli were matched on sound duration (750 ms), triad structure (e.g. three tones, three CV pairs, and three-syllable words), average intensity (70 dB SPL), percent of target trials (25%), and difficulty of task instructions (2-fold discrimination task). The tone stimuli also had a fixed onset for the second and third tones, 250 and 500 ms, respectively (this was easy to do without distorting the sound because the tones were synthesized). In contrast, the second and third CV pairs began on average at 230 ms and 455 ms, respectively; and the second and third syllables began at 210 ms and 432 ms, respectively. Stimuli for the phonological and semantic conditions were further matched as closely as possible on both syllable-initial and syllable-medial phonemic content. Additional consideration was taken during the recording of the CV triplets and words to try and match them on prosody. This was accomplished by using a carrier phrase and by alternating the recording between CV triplet and word stimuli while trying to make the delivery as similar as possible.

### ***Tone trains***

The tone trains consisted of three pure tone sine waves of 500 Hz, 600 Hz, 700 Hz, 800 Hz, 900 Hz, and 1000 Hz synthesized in Audacity (<http://audacity.sourceforge.net/>) and concatenated in Nero WaveEditor (<http://www.nero.com>). A sound intensity onset



and offset ramp was imposed on the tone stimuli in order to match the natural ramps in the voice-recorded CV triplet and word stimuli. The natural fade-in time was measured for the CV triplet and word stimuli by taking an average of the times it took the stimuli to reach 75% of maximum amplitude of the first vowel. The fade-out time was similarly measured by taking the average of the difference between the times it took the stimuli to reach 75% of the maximum amplitude of the last vowel, and the full duration of the sound (750ms). The calculated fade-in and fade-out times, 90 ms and 166 ms respectively, were then applied to the tone-train stimuli using Audacity's fade-in and fade-out features.

### ***Word stimuli***

The three-syllable word stimuli were recorded in a soundproof recording room by a native English-speaking male, and all words were three syllables long. In order to maximize the number of trials, the word stimuli were selected from categories which yielded the highest number of three-syllable words. Ultimately, the largest lists of words fit into 1 of 4 categories: plants, animals, foods, and occupations. Ideally, all word stimuli would have come from the animal category as in the Binder et al. studies, but because we were constrained to three-syllable words, this could not have been achieved without drastically reducing the number of trials or using repeating or very obscure stimuli. Words were syllabified using the maximal onset principle (Pulgram, 1970) that states: "When there is ambiguity between 1 syllable's coda and the onset of the next syllable that consonant should be attached to the onset of the next syllable" (Titone & Connine, 1997, p. 2). This made the most sense as we wanted to better capture the consonant sounds and apply their phonemic content to the CV triplet stimuli. Furthermore, Titone &

Connine (1997) showed this syllabification strategy is more operative in auditory word recognition, thus suggesting this is the brain’s preferential way of segmenting aurally presented words.

***Consonant-vowel (CV) triplets***

The list of CV triplets was created by randomly pairing consonants and vowels together to match as closely as possible the distribution of phoneme type (e.g. voicing and place of articulation) with the word stimuli. The vowels were evenly distributed across /æ/, /i/, /a/, /o/, /u/. For the phonological task /p/ and /t/ were chosen as the target sounds, which participants were required to respond if they heard both in the same sequence. Finally, the structure of the CV triplets was constrained to fit into 1 of 6 structure sets to ensure the following (see Table 1):

- 1) 25% of trials were targets
- 2) of the target trials, all six possible configuration types were equally represented
- 3) all non-target trial configurations were equally represented

Table 1. CV Triplet Structure Sets

<b>A</b>				<b>B</b>			
?	/p/	/t/	6	?	?	/p/	18
?	/t/	/p/	6	?	?	/t/	18
/p/	/t/	?	6	?	/p/	?	18
/p/	?	/t/	6	?	/t/	?	18
/t/	/p/	?	6	/p/	?	?	18
/t/	?	/p/	6	/t/	?	?	18
36				108			

*Note.* **A**, Target structures, and **B**, Non-targets structures. The ‘?’ represents a randomly assigned phoneme other than /p/ or /t/ taken from a pool of phonemes present in the word stimuli.

## Procedure

At the time of the experiment, participants completed the Edinburgh Handedness Inventory (EHI) to assess their degree of hand dominance (Oldfield, 1971). They were then fitted with a 256-channel Hydrocel Geodesic Sensor Net for EEG recording and seated in front of a computer monitor. A chin rest was used to maintain a fixed distance from the monitor and minimize head movement. Participants then focused on a white fixation cross overlaid on a black computer screen while stimuli were presented binaurally for all 3 conditions in a standard block design. The inter-trial interval was approximately three seconds long with 500-1000 ms jitter at the start of each trial (in order to prevent anticipation), followed by 750 ms of stimulus presentation, and then 1500 ms to respond (see Figure 1). To address the possibility of order effects, participants received 1 of 6 different counterbalanced block sets. Each set was composed of twelve 36-trial blocks: four acoustic, four semantic and four phonological.

The three separate tasks associated with the three conditions all used a go-no-go paradigm in which the participant responded to targets with a button press using their left index finger. Task instructions required participants to keep in mind 2 separate criteria (different for each of the 3 conditions) which determined when it was appropriate to respond. Participants were given instructions for all the tasks before the experiment began so they could ask questions. This design was modeled after the Binder et al., (1995, 2008) fMRI studies. In the acoustic blocks participants listened to a tone train and were instructed to respond if they believed the first and the last (third) tone were the same pitch, and higher in pitch than the middle (second) tone. In the phonological blocks participants listened to CV triplets and were instructed to respond if they heard both /p/

and /t/ sounds within the CV triplet. There were four separate categories and tasks associated with the four semantic blocks, one for each block. In each block participants listened to 36 words from one of the following categories (animals, plants, foods, and occupations). In the animal block, participants were instructed to respond if they believed the animal was found in the United States and could fly. In the plant block, participants were instructed to respond if they believed the plant to be a fruit and commonly found in a North American home garden. In the food block, participants were instructed to respond if they believed the food was of Italian cuisine and predominantly contained animal products (including dairy and eggs). In the occupation block, participants were instructed to respond if they believed the occupation was white collar and often called for a post-bachelor's (graduate) degree.

At the end of the experiment participants were presented with a screen informing them they had completed the experiment. Participants were then given a copy of the consent form they had signed at the beginning of the experiment. Lastly, they were thanked and given \$30 remuneration for their participation.

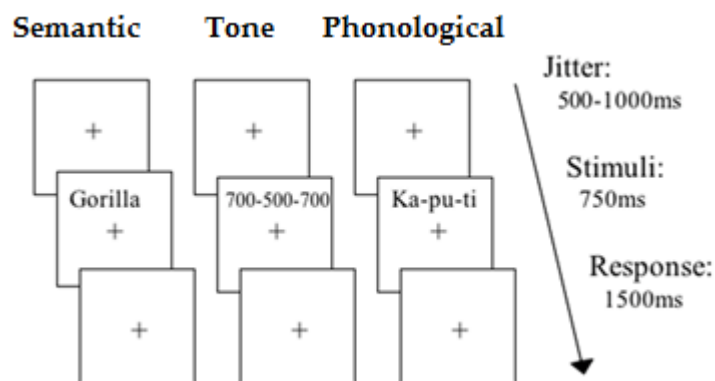


Figure 1. Trial Design. All 3 conditions used the same trial design.

## **Design**

### **Rationale and independent variables**

As previously noted, the three experimental conditions, acoustic decision, phonological decision, and semantic decision, were modeled after the Binder et al. (2008) fMRI study and had the following characteristics and rationale. The acoustic decision condition required processes related to the acoustic aspects of the stimulus. The phonological decision task required processing of acoustic, as well as phonological properties of the stimulus. The semantic decision task required processing of acoustic, phonological, and semantic properties of the stimulus. All three conditions were active, rather than passive; specifically, they required focused attention on relevant aspects of the stimuli, holding task instructions in mind, making a decision, and generating a motor response (Binder et al., 2008). The latter 3 processes are considered general process, are nonlinguistic, and should not be considered in the mapping of language functioning. By placing equal demands on these general functions in all conditions and focusing the analysis on condition differences, processing activity specifically related to language functioning (e.g., phonology and semantics) could be better separated from non-linguistic processing activity.

### **EEG recording and preprocessing**

The EEG was acquired with a 256-channel HydroCel Geodesic Sensor Net, Net Amps 300 amplifier, and Net Station, version 4.5 software (Electrical Geodesics, Eugene, OR). Electrode impedances were maintained below 100 kOhms, and all channels were referenced to Cz during acquisition. The EEG was recorded with a DC amplifier at a gain

of 1,000, sampled at a rate of 500 Hz, and digitized with a 24-bit analog-to-digital converter.

After acquisition, the continuous EEG was filtered from 0.1 to 30 Hz, and segmented into 1,700-ms stimulus-locked epochs from 200 ms pre-stimulus to 1500 ms post-stimulus. Epochs contaminated with eye or movement artifact, as identified by computerized algorithm (e.g. 110  $\mu$ V difference between EEG channels above and below the eyes for blinks and 100  $\mu$ V difference between EEG channels near the outer canthi for lateral eye movements) and visual inspection, were eliminated. Individual bad channels were replaced on a segment-by-segment basis with spherical spline interpolation (Perrin, Pernier, Bertrand, Giard, & Echallier 1987). Individual ERP averages were computed separately for each experimental condition: Semantic, Phonological, and Tone. The average ERPs were re-referenced to an average reference with polar average reference effect (PARE) correction to estimate the zero surface potential integral, (Junghofer, Elbert, Tucker, & Braun, 1999) and adjusted to a 100-ms prestimulus baseline.

### **Measures**

Seven ERP peaks were examined: the P1-N1-P2 auditory evoked potentials, the N365 and N480 peaks around the N400 window, the late positive complex (LPC), and a late anterior ventral positivity (LAVP). The time windows for each ERP were as follows: 34-78 ms for the P1, 80-156 ms for the N1, 148-280 ms for the P2, 285-381 ms for the N365, 416-546 ms for the N480, 642-950 ms for the LAVP, and 550-1100 ms for the late positive component (LPC) and late frontal negativity (LFN). Amplitudes were measured using an adaptive mean centered on the peak within an appropriate time-window based on the grand average for each electrode. The adaptive means for each component were

computed as follows: 10-ms window centered on the peak of the P1; 20-ms window centered on the peak of the N1, P2, N365, and N480; 40-ms window centered on the LPC peak; and a 30-ms window centered on the LAVP peak. Appropriate electrode groups were identified to best capture each ERP component (see Figure 2), and sub-grouped into left, midline, and right electrode sites (except the lateral anterior ventral positivity, which had only left and right electrode subgroups). Then, for each electrode group an average of the adaptive mean amplitudes computed within the electrodes of that group was computed and served as the dependent variables in the analyses described next.

All ERP components were analyzed using a repeated measures analysis of variance with up to three within subjects factors (see Results section for exact factors per ERP analysis): an experimental condition factor, consisting of three levels (acoustic, phonological, and semantic) for the early ERPs (P1, N1, P2), and two levels (only phonological and semantic) for the mid and later ERPs; a laterality factor consisting of three levels (left, midline, and right) except for the LAVP (only left and right); and a location factor of up to 3 levels depending on the topography of the ERP component (anteroventral, frontopolar, frontocentral, central, centroparietal, parietal, occipital). The acoustic condition was not included in the analyses of ERP components beyond the P2, because its stimulus characteristics were too different from the semantic and phonological condition stimuli. Specifically, the three tones within the tone trains were exactly 250 ms apart for each stimulus which allowed for strong superimposed P1-N1-P2 complexes to the second and third tones in the tone train which overshadowed later ERP components.

## **Contrasts**

The design of this study allows for two important contrasts. The first contrasts the semantic decision vs. the tone decision task in order to isolate language-specific processes (phonological and semantic), while ignoring simple acoustic processes, as well as general attention and decision making processes. This first contrast can be used to determine the lateralization of language for an individual. In fMRI studies, a laterality index (LI) can be computed for each subject and task contrast using the formula  $(L - R)/(L + R)$ , where L and R are the number of significant voxel activations in the left and right hemispheres of the brain. However, this contrast and subsequent analysis were not conducted because of the unique characteristics of the tone condition previously mentioned. This means a lateralization index, comparable to the Binder et al., 2008 study will not be calculated. However, lateralization of language is a crude measurement and localization of the language conditions is more important. The second contrasts the semantic decision vs. the phonological decision task, in order to isolate semantic processing, while ignoring acoustic, phonological, general attention, working memory, and decision-making processes. For the current study, the semantic - phonological contrast was accomplished using t-test waves, plotting the resulting t values (from a Student's t test) as a function of time across all 256 sensor locations.

## **Source estimates**

Source estimates, describing cortical generators of measured scalp potentials, were accomplished using GeoSource, version 2.0 software (Electrical Geodesics, Eugene, OR). To compute source estimates, a linear inverse minimum norm solution with standardized low resolution brain electromagnetic tomography constraint (sLORETA;



Pascual-Marqui, 2002) was used on the grand-averaged scalp ERPs and the resulting semantic – phonological t-test wave. A finite difference model (FDM) was used to more accurately compute the lead field in relation to head tissues. The FDM head model was constructed from a whole-head computed tomography (CT) and MRI scans (Colin27) for tissue segmentation of a single individual, whose Talairach-transformed head geometry closely matched that of the Montreal Neurological Institute (MNI305) average (Holmes et al., 1998). Conductivity values used in the FDM model are as follows: 0.25 S/m (Siemens/meter) for brain, 1.8 S/m for cerebral spinal fluid, 0.018 S/m for skull, and 0.44 S/m for scalp (Ferree et al., 2000). Dipole placement is based on the probabilistic map of the MNI305 average brain. Informed by the probabilistic map, cortical gray matter was parceled into 7 mm voxels, each serving as a source location with three orthogonal orientations. This resulted in a total of 2,447 source dipoles, each with x, y, and z orientations. The resulting estimated dipole source activations were visualized by superimposing them on MRI slice views of the Talairach-transformed Colin27 brain. Source localization was carried out around time points of significant scalp differences between phonological and semantic conditions. For each ERP of interest, sources were thresholded such that only the top 70% of voxel intensities were displayed on MRI slice views of a Talairach-transformed brain.

## CHAPTER III

### RESULTS

#### **Event-Related Potentials (ERPS)**

Grand average ERPs for semantic, phonological, and acoustic conditions from -200 ms (baseline period) to 1500 ms post stimulus can be seen in Figure 3. Mean amplitude for each ERP component for each cell is provided in Table 2.

#### **P1-N1-P2 complex**

The P1, N1, and P2 auditory ERP components were measured from central electrode sites (colored purple in figure 2). A condition (acoustic, phonological, semantic) x laterality (left, mid, right) within-subjects ANOVA was conducted separately on each component. Waveforms for the P1-N1-P2 over central locations can be seen in figure 4 and topomaps can be seen in figure 5.

#### ***P1 latency window (34—78 ms)***

There were no significant experimental condition differences for the P1 amplitude. The ANOVA revealed a main effect for the laterality factor  $F(2, 46) = 5.99, p = .005; \eta p^2 = 2.07$ . Mauchly's test of sphericity for laterality indicated the assumption of sphericity had not been violated ( $\chi^2(2) = 2.72, p = .257$ ). The P1 was largest over the midline ( $M = 0.97 \mu V, SE = 0.07$ ), smaller over the right hemisphere ( $M = 0.86 \mu V, SE = 0.07$ ), and the smallest over the left hemisphere ( $M = 0.82 \mu V, SE = 0.05$ ). Bonferroni adjusted pairwise comparisons of laterality revealed that the difference in P1 amplitude

over the midline compared to left hemisphere sites was significant ( $M = 0.15 \mu\text{V}$ ,  $SE = 0.40$ ),  $p = .003$ . No other comparisons were significantly different.

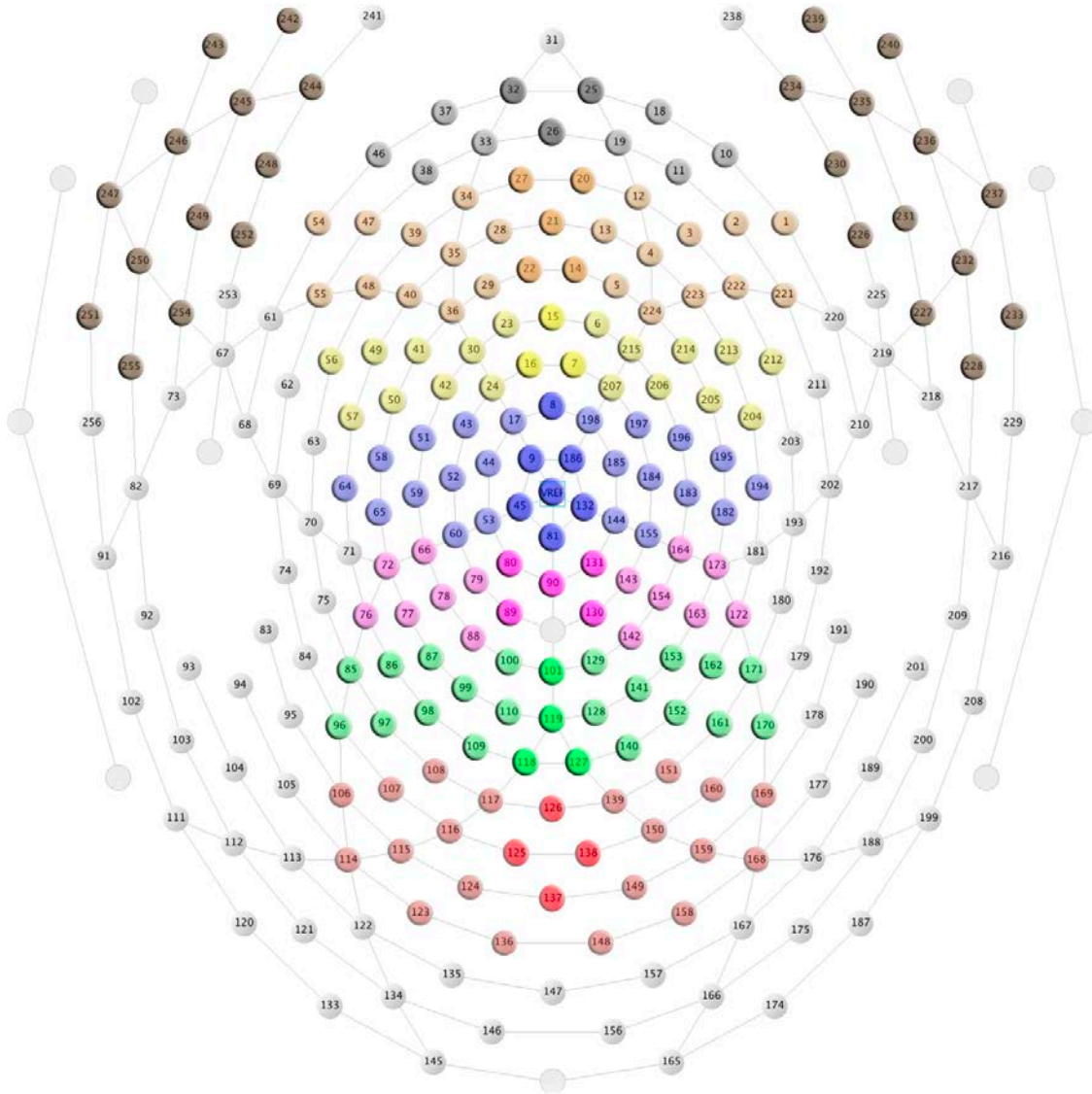


*Figure 2.* ERP Electrode Groupings: anteroventral (brown; LAVP), frontopolar (gray; P365), frontal (orange; P365, LFN), frontocentral (yellow; LFN), central (blue; P1, N1, P2), centroparietal (purple; N365, N480, LPC), parietal (green; N365, N480, LPC), and occipital (red; N365). All electrode groups were further subdivided into left, middle, and right groups, except the anteroventral which has only left and right subgroups. The darker colors down the midline represent the midline electrode groups, and separate left and right groups are shaded in lighter colors.

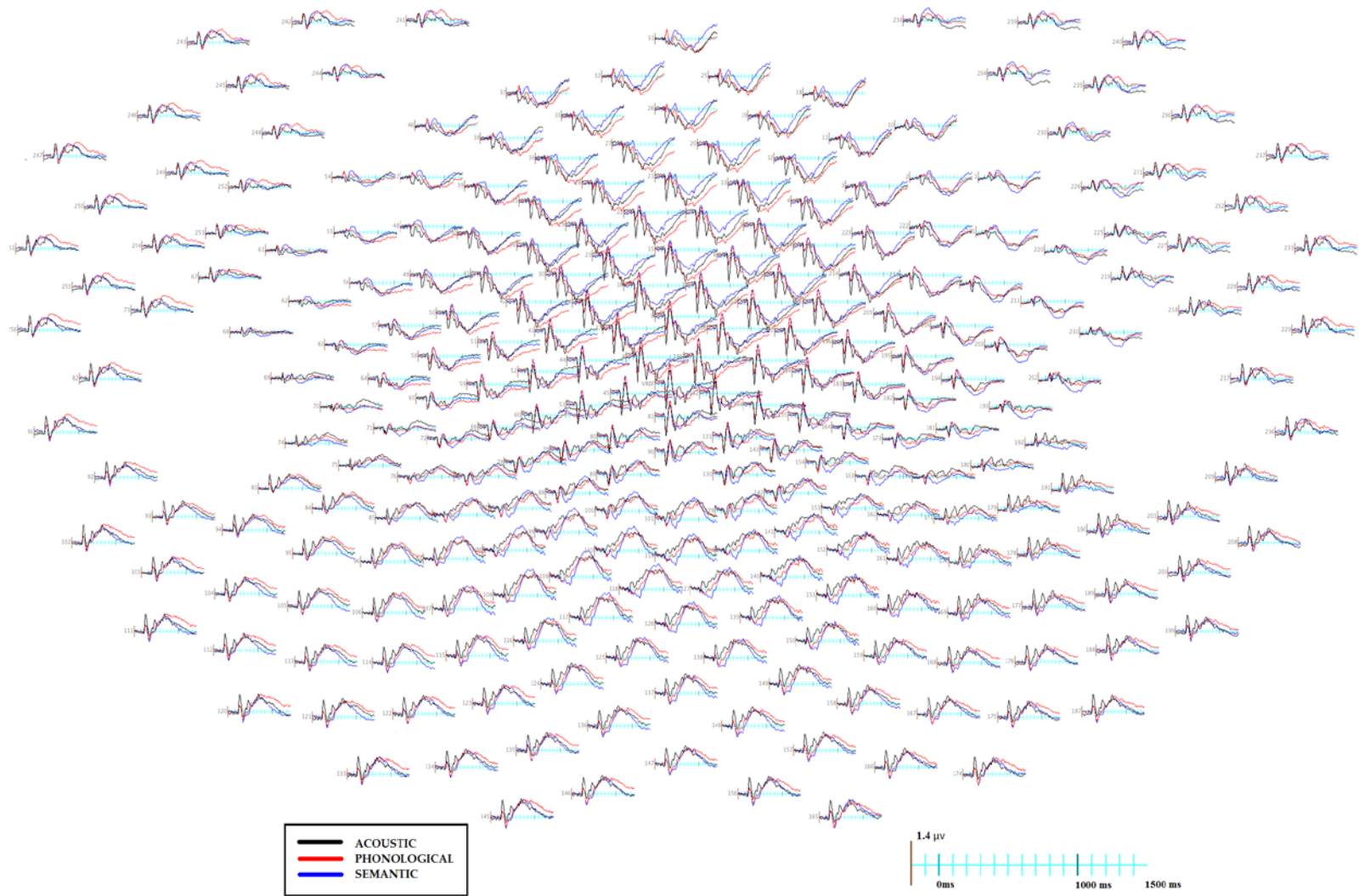


Figure 3. Grand Average ERPs. ERPs are plotted from -200 to 1500 ms, positive plotted up, for all experimental conditions.

Table 2. Mean Amplitudes ( $\mu V$ ) and Standard Deviations for All ERPs at All Measured Electrode Sites.

ERP	Electrode Groups	Tone			Phoneme			Semantic		
		Left	Midline	Right	Left	Midline	Right	Left	Midline	Right
		Mean (SD)	Mean (SD)	Mean (SD)	Mean (SD)	Mean (SD)	Mean (SD)	Mean (SD)	Mean (SD)	Mean (SD)
<b>P1</b>	Central	0.83 (.08)	1.01 (.10)	0.90 (.08)	0.73 (.06)	0.91 (.09)	0.84 (.08)	0.83 (.07)	0.97 (.08)	0.85 (.07)
<b>N1</b>	Central	-3.60 (1.29)	-4.54 (1.45)	-3.72 (1.30)	-2.26 (1.04)	-2.94 (1.28)	-2.35 (1.00)	-2.24 (0.89)	-2.98 (1.17)	-2.55 (0.95)
<b>P2</b>	Central	1.30 (1.66)	2.45 (2.19)	1.59 (1.51)	2.31 (1.78)	3.46 (2.29)	2.67 (1.88)	2.38 (1.74)	3.61 (2.09)	2.66 (1.86)
	CentroParietal	-	-	-	-1.31 (1.42)	-1.48 (1.85)	-0.84 (1.24)	-1.99 (1.28)	-2.4 (1.93)	-1.35 (1.38)
<b>N365</b>	Parietal	-	-	-	-0.54 (0.96)	-0.50 (1.01)	-0.55 (0.89)	-1.60 (1.11)	-1.96 (1.40)	-2.02 (1.29)
	Occipital	-	-	-	-0.51 (1.20)	-0.65 (1.05)	-0.67 (1.12)	-1.35 (1.38)	-1.86 (1.28)	-1.69 (1.24)
<b>P365</b>	Frontopolar	-	-	-	0.49 (1.31)	0.44 (1.56)	0.70 (1.51)	1.56 (1.88)	1.47 (1.88)	1.56 (1.62)
	Frontal	-	-	-	-0.08 (1.37)	-0.19 (1.61)	0.40 (1.43)	0.75 (1.46)	0.56 (1.76)	0.77 (1.49)
<b>N480</b>	CentroParietal	-	-	-	-1.14 (1.46)	-1.47 (2.13)	-1.18 (1.51)	-1.99 (1.39)	-2.16 (2.01)	-2.2 (1.48)
	Parietal	-	-	-	0.23 (1.33)	0.39 (1.78)	-0.12 (1.52)	-0.69 (1.32)	-0.66 (1.45)	-1.22 (1.29)
<b>LAVP</b>	AnteroVentral	-	-	-	2.65 (.32)	-	2.14 (.36)	1.55 (.26)	-	1.06 (.25)
<b>LPC</b>	Parietal	-	-	-	3.35 (1.26)	3.71 (1.4)	2.68 (1.19)	4.2 (1.88)	4.66 (2.05)	3.16 (1.55)
	CentroParietal	-	-	-	1.33 (1.42)	1.29 (1.86)	0.86 (1.34)	1.99 (1.56)	2.19 (1.54)	1.05 (1.28)
<b>LFN</b>	Frontal	-	-	-	-4.69 (1.92)	-5.96 (2.39)	-4.77 (1.62)	-3.77 (1.79)	-4.08 (2.16)	-4.26 (1.71)
	FrontoCentral	-	-	-	-4.55 (2.03)	-6.02 (3.14)	-4.56 (1.9)	-3.75 (1.84)	-4.27 (2.48)	-4.28 (1.78)

### ***N1 latency window (80—156 ms)***

Mauchly's test of sphericity for condition indicated that the assumption of sphericity had been violated  $\chi^2(2) = 19.9, p < .001$ . Therefore, degrees of freedom were corrected using Greenhouse-Geisser estimates of sphericity ( $\epsilon = 0.63$ ). The N1 for the acoustic condition ( $M = -3.95 \mu\text{V}, SE = 0.26$ ) was much larger than either the phonological ( $M = -2.52 \mu\text{V}, SE = 0.21$ ) or semantic condition ( $M = -2.59 \mu\text{V}, SE = 0.20$ ),  $F(1.25, 75.3) = 45.5, p < .001; \eta^2 = 0.66$ . Bonferroni adjusted pairwise comparisons showed there was a significant difference in N1 amplitude for the acoustic condition vs. the phonological condition ( $M = -1.44 \mu\text{V}, SE = 0.19$ ),  $p < .001$ , and vs. the semantic condition ( $M = -1.37 \mu\text{V}, SE = 0.21$ ),  $p < .001$ . Furthermore, the ANOVA for N1 amplitude revealed a main effect of laterality, showing the N1 was largest over the midline,  $F(2, 12.2) = 25.7, p < .001; \eta^2 = 0.53$ . Bonferroni adjusted pairwise comparisons showed there was a significant difference in N1 amplitude at the midline compared to the left hemisphere electrode group ( $M_{diff} = -0.78 \mu\text{V}, SE = 0.10$ ),  $p < .001$ , and the right hemisphere electrode group ( $M_{diff} = -0.61 \mu\text{V}, SE = 0.13$ ),  $p < .001$ .

### ***P2 latency window (148—280 ms)***

Mauchly's test of sphericity indicated that the assumption of sphericity had been violated for both experimental condition  $\chi^2(2) = 9.56, p = .008$ , and for laterality  $\chi^2(2) = 7.75, p = .021$ . Therefore, degrees of freedom were corrected using Greenhouse-Geisser estimates of sphericity ( $\epsilon = 0.74$  and  $0.77$  respectively). There was a main effect for experimental condition  $F(1.48, 36.9) = 18.5, p < .001; \eta^2 = 0.45$ . There was also a main effect for laterality  $F(1.54, 34.8) = 26.9, p < .001; \eta^2 = 0.54$ . P2 amplitude for the acoustic condition ( $M = 1.78 \mu\text{V}, SE = 0.35$ ) was smaller than the phonological ( $M = 2.81$

$\mu\text{V}$ ,  $SE = 0.39$ ) and semantic conditions ( $M = 2.88 \mu\text{V}$ ,  $SE = 0.37$ ). Bonferroni adjusted pairwise comparisons showed the P2 amplitude for the acoustic condition was significantly smaller than the phonological ( $M_{diff} = -1.03 \mu\text{V}$ ,  $SE = 0.24$ ),  $p < .001$  and semantic conditions ( $M_{diff} = -1.1 \mu\text{V}$ ,  $SE = 0.22$ ),  $p < .001$ . There were no significant differences between phonological and semantic conditions. Again, the main effect of laterality shows enhanced P2 amplitude at the midline ( $M = 3.17 \mu\text{V}$ ,  $SE = 0.42$ ) compared to left ( $M = 2.0 \mu\text{V}$ ,  $SE = 0.33$ ) and right ( $M = 2.31 \mu\text{V}$ ,  $SE = 0.34$ ) hemisphere electrode groups. Bonferroni adjusted pairwise comparisons showed that P2 amplitude at the midline was significantly less than left hemisphere ( $M_{diff} = 1.18 \mu\text{V}$ ,  $SE = 0.19$ ),  $p < .001$ , and right hemisphere ( $M_{diff} = 0.87 \mu\text{V}$ ,  $SE = 0.19$ )  $p < .001$  electrode groups.

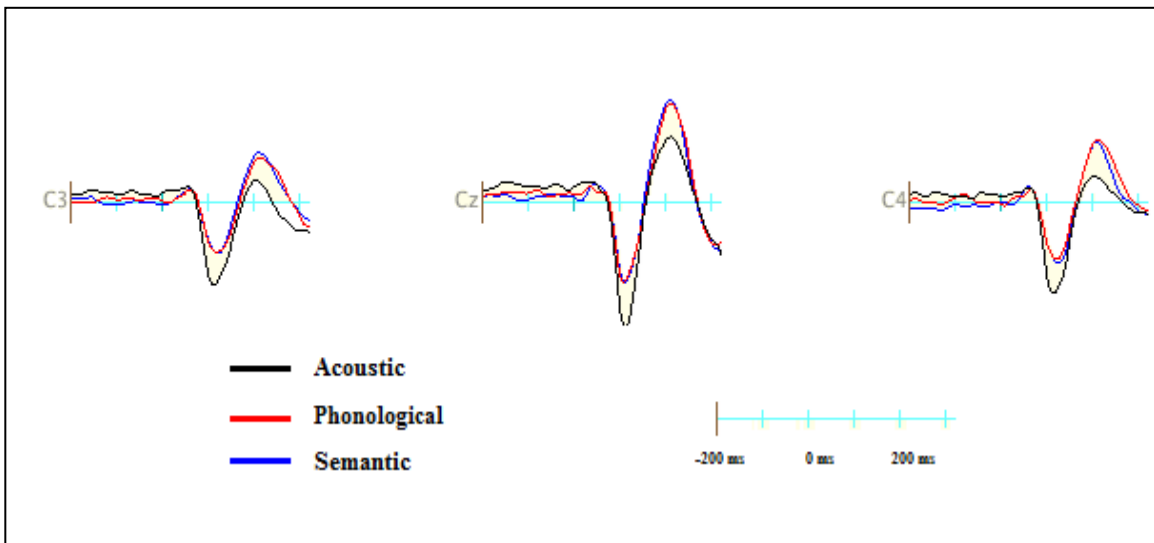


*Figure 4.* P1-N1-P2 Complex Waveforms. ERP waveforms are shown at central scalp locations from 200 ms before stimulus onset and 300 ms after.

## **N400-window components**

### *N365 latency window (285—382 ms)*

The N365 was the first N400-like component. This component was measured from centroparietal, parietal and occipital electrode sites (colored blue, purple, and green respectively in figure 2). A condition (phonological, semantic) x location (centroparietal, parietal, occipital) x laterality (left, mid, right) within subjects ANOVA was conducted on the adaptive mean amplitudes. A main effect of condition indicated that the N365 was larger for the semantic condition ( $M = -1.89 \mu\text{V}$ ,  $SE = 0.17$ ) compared to the phonological condition ( $M = -1.78 \mu\text{V}$ ,  $SE = 0.21$ ),  $F(1,23) = 56.2$ ,  $p < .001$ ;  $\eta^2 = 0.71$ .

There were also several interactions, including a significant interaction between laterality and experimental condition,  $F(2,46) = 6.74$ ,  $p = .003$ ;  $\eta^2 = 0.23$ , a significant interaction between location and laterality, Greenhouse-Geisser corrected ( $\epsilon = .55$ ),  $F(3.97,23.6) = 3.87$ ,  $p = .006$ ;  $\eta^2 = 0.14$ , and a three-way interaction across condition, location, and laterality factors,  $F(2.87,66.1) = 5.02$ ,  $p = .004$ ;  $\eta^2 = 0.18$ . These interactions can be explained by the N365 for the semantic condition being larger over midline ( $M = -2.07 \mu\text{V}$ ,  $SE = 0.24$ ) and right ( $M = -1.95 \mu\text{V}$ ,  $SE = 0.22$ ) electrode groups for all location factors compared to left ( $M = -1.65 \mu\text{V}$ ,  $SE = 0.20$ ) electrode groups. In contrast, the N365 for the phonological condition was more evenly distributed across laterality factors at centroparietal and occipital scalp locations. However, the N365 for the phonological condition at parietal sites was much larger over left ( $M = -1.31 \mu\text{V}$ ,  $SE = 0.29$ ) and midline ( $M = -1.48 \mu\text{V}$ ,  $SE = 0.38$ ) groups compared to the right ( $M = -0.84 \mu\text{V}$ ,  $SE = 0.25$ ) hemisphere sites.



*N480 latency window (416—546 ms)*

The N480 was the second N400-like component. This component was measured from centroparietal and parietal electrode sites (colored in blue and purple in Figure 2). A condition (phonological, semantic) x location (centroparietal, parietal) x laterality (left,

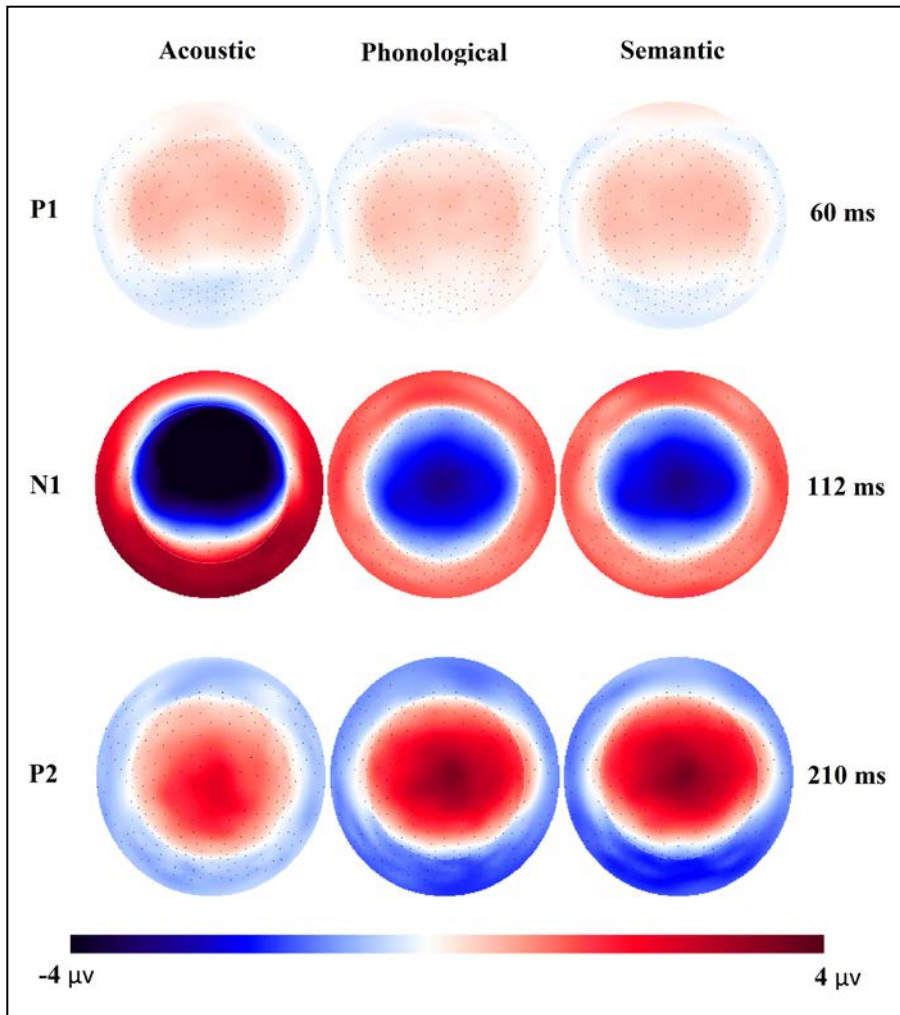


*Figure 5.* P1-N1-P2 Complex Topographical Maps. The topographic maps show the full topography during the peaks of the P1-N1-P2 complex.

mid, right) within subjects ANOVA was conducted on the adaptive mean amplitudes.

Like the N365, a main effect of condition revealed that the N480 was larger (more negative) for the semantic condition ( $M = -1.49 \mu\text{V}$ ,  $SE = 0.26$ ) than for the phonological condition ( $M = -0.55 \mu\text{V}$ ,  $SE = 0.28$ ), collapsed across all other factors  $F(1, 23) = 13.1$ ,  $p$

= < .001;  $\eta^2 = 0.36$ . Unlike the N365, a main effect of location revealed the N480 was found to be largest over centroparietal ( $M = -1.69 \mu\text{V}$ ,  $SE = 0.29$ ) vs. parietal ( $M = -0.35 \mu\text{V}$ ,  $SE = 0.24$ ) electrode groups  $F(1,23) = 4.2$ ,  $p = < .001$ ;  $\eta^2 = 0.57$ . There was also a significant interaction between location and laterality factors for which Mauchly's test of sphericity indicated the assumption of sphericity had been violated  $\chi^2(2) = 19.9$ ,  $p < .001$ . Therefore, degrees of freedom were corrected using Greenhouse-Geisser estimates of sphericity ( $\epsilon = 0.63$ ),  $F(2,46) = 5.9$ ,  $p = .016$ ;  $\eta^2 = 0.20$ . In both experimental conditions, and only at parietal electrode sites, the N480 amplitude was larger at right hemisphere sites while left and midline groups were about the same. At centroparietal sites the N480 amplitude was smallest at left hemisphere sites and largest at midline and right hemisphere sites, which were approximately the same amplitude.

### ***P365 latency window (285—382 ms)***

The P365 appeared to be the inversion of the first N400-like component, the N365, as its time course was nearly identical, suggesting the same generator. The P365 was measured from frontopolar and frontocentral electrode groups (colored gray and yellow in Figure 2). A condition (phonological, semantic) x location (frontopolar and midfrontal) x laterality (left, mid, right) within subjects ANOVA was conducted on the adaptive mean amplitudes. The amplitude of the P365 was larger for the semantic condition ( $M = 1.11$ ,  $SE = 0.31$ ) than the phonological condition ( $M = 0.29$ ,  $SE = 0.26$ ) as indicated by the main effect of experimental condition,  $F(1,23) = 12.1$ ,  $p = .002$ ;  $\eta^2 = 0.35$ . The P365 was found to be largest over frontopolar electrode groups  $F(1,23) = 8.42$ ,  $p = .008$ ;  $\eta^2 = 0.27$  collapsed across all other factors. There were two significant interactions, one between experimental conditions and location factors,  $F(1,23) = 4.59$ ,  $p$

=.043;  $\eta^2 = 0.17$ , and the other between the location and laterality factors,  $F(2,46) = 3.87$ ,  $p = .028$ ;  $\eta^2 = 0.14$ . The former interaction seemed to reflect the increase in amplitude for the P365 in semantic condition at frontopolar sites, compared to mid-frontal sites, which was larger than the phonological condition. Nevertheless, this interaction can likely be accounted for by the latter interaction which highlights the increased amplitude for the P365 in the phonological condition over the right hemisphere, which was particularly right lateralized in the frontocentral electrode group.

### **Late components**

#### ***Late positive complex (LPC) latency window (600—900 ms)***

Data from one extreme outlier was removed from analysis of the LPC. The LPC was measured from centroparietal and parietal electrode groups (colored purple and green in figure 2). A condition (phonological, semantic) x location (centroparietal, parietal) x laterality (left, mid, right) within subjects ANOVA was conducted on the adaptive mean amplitudes. The LPC for the semantic condition ( $M = 4.01$ ,  $SE = 0.36$  at parietal sites,  $M = 1.74$ ,  $SE = 0.26$  at centroparietal sites) was significantly larger than the LPC for the phonological condition ( $M = 3.25$ ,  $SE = 0.23$  at parietal sites and,  $M = 1.16$ ,  $SE = 0.26$  at centroparietal sites,  $F(1, 22) = 4.81$ ,  $p = .039$ ;  $\eta^2$ . The LPC was significantly larger over parietal scalp locations than over centroparietal scalp locations,  $F(1, 22) = 78.7$ ,  $p < .001$ ;  $\eta^2=0.78$ . The LPC was also found to be larger over the left hemisphere ( $M = 2.72$ ,  $SE = 0.27$ ) and midline ( $M = 2.96$ ,  $SE = 0.24$ ), and significantly smaller over the right hemisphere ( $M = 1.94$ ,  $SE = 0.20$ )  $F(1.53, 33.6) = 11.8$ ,  $p < .001$ ;  $\eta^2=.78$ . Mauchly's test of sphericity indicated the assumption of sphericity had been violated for the laterality

factor,  $\chi^2(2) = 19.9, p < .001$ . Thus, degrees of freedom were corrected using Greenhouse-Geisser estimates of sphericity ( $\epsilon = 0.63$ ).

***Late anterior ventral positivity (LAVP) latency window (642—950 ms)***

The LAVP was measured from anteroventral electrode groups (colored brown in figure 2). A condition (phonological, semantic) x laterality (left, right) within subjects ANOVA was conducted on the adaptive mean amplitudes. The late anterior ventral positivity was significantly larger for the phonological condition ( $M = 2.4, SE = 0.33$ ) than for the semantic condition ( $M = 1.3, SE = 0.25$ ) over both left and right hemispheres,  $F(1,23) = 14.1, p = .001; \eta^2 = 0.38$ . The late anteroventral positivity was significantly larger over the left hemisphere ( $M = 2.1, SE = 0.25$ ) than the right hemisphere ( $M = 1.6, SE = 0.27$ ) across both experimental conditions  $F(1,23) = 5.95, p = .002; \eta^2 = 0.35$ . There was no significant interaction between condition and laterality factors  $F(1,23) = 0.01, p > .05$ .

***Late frontal negativity (LFN) latency window (550—1100 ms)***

The late frontal negativity was measured from frontal and centrofrontal electrode groups (colored orange and brown in figure 2). A condition (phonological, semantic) x location (frontal, centrofrontal) x laterality (left, mid, right) within subjects ANOVA was conducted on the adaptive mean amplitudes. The late frontal negativity was larger (more negative) for the phoneme condition compared to the semantic condition,  $F(1,23) = 14.9, p < .001; \eta^2 = 0.39$ . There was a main effect for laterality,  $F(2, 46) = 9.1, p < .001; \eta^2 = 0.284$ . This effect shows that late frontal negativity is larger over the midline ( $M = -5.08, SE = 0.48$ ) than either left ( $M = -4.19, SE = 0.36$ ) or right ( $M = 4.47, SE = 0.33$ ) hemisphere groups. Bonferroni adjusted pairwise comparisons revealed that the

difference in amplitudes of the late frontal negativity at the midline compared to either the left hemisphere ( $M = -0.89$ ,  $SE = 0.28$ ) or the right hemisphere electrode groups ( $M = -0.62$ ,  $SE = 0.23$ ) was significant,  $p = .002$  and  $p = .042$  respectively. The difference between left and right hemisphere groups was not significant. There was also a significant interaction between experimental condition and laterality factors,  $F(2,46) = 26.3$ ;  $\eta^2 = 0.53$ . This effect seems to suggest that the late frontal negativity is strongly focused at the midline for the phonological condition, and the late frontal negativity is equally as strong at midline and right electrode groups, but is weaker at left hemisphere sites for the semantic condition.

Phonological and semantic condition topomaps for the N400-window and later components can be seen in figure 6. Overlaid grand average ERP waveforms (phonological and semantic conditions) can be seen for all N400-window and later ERP components from posterior and anterior electrode sites (See Figure 7 and Figure 8)

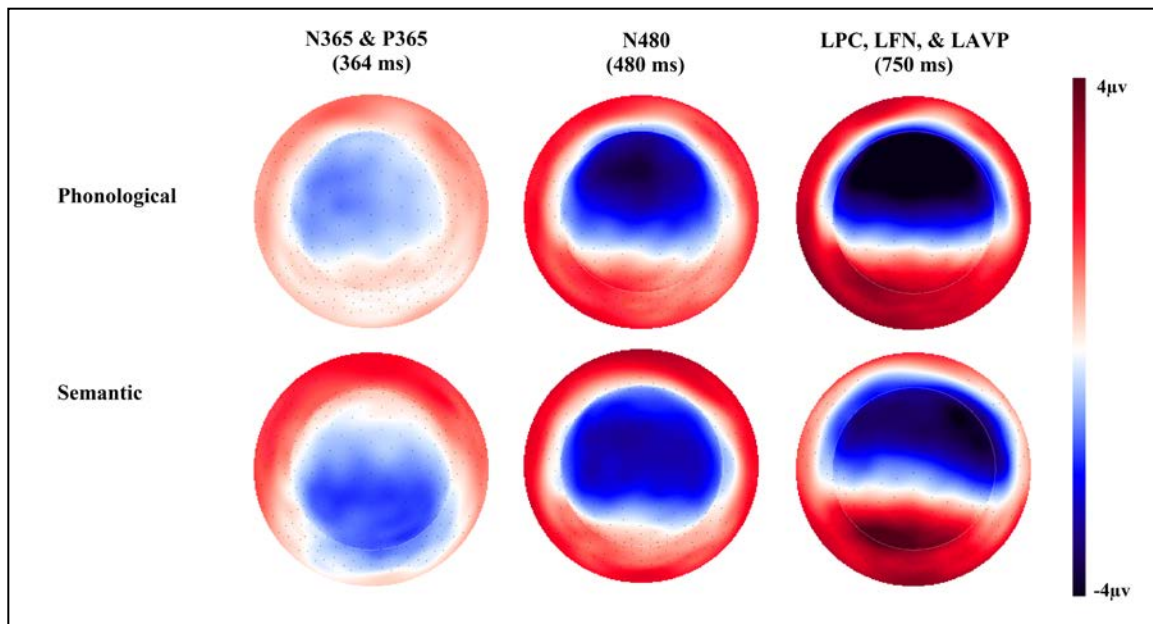


*Figure 6.* N400-Window and Later Component Topographic Maps. The topographic maps show the full topography during the peaks of the N365, N480, and LAVP, and the first peak of the LPC/LFN.

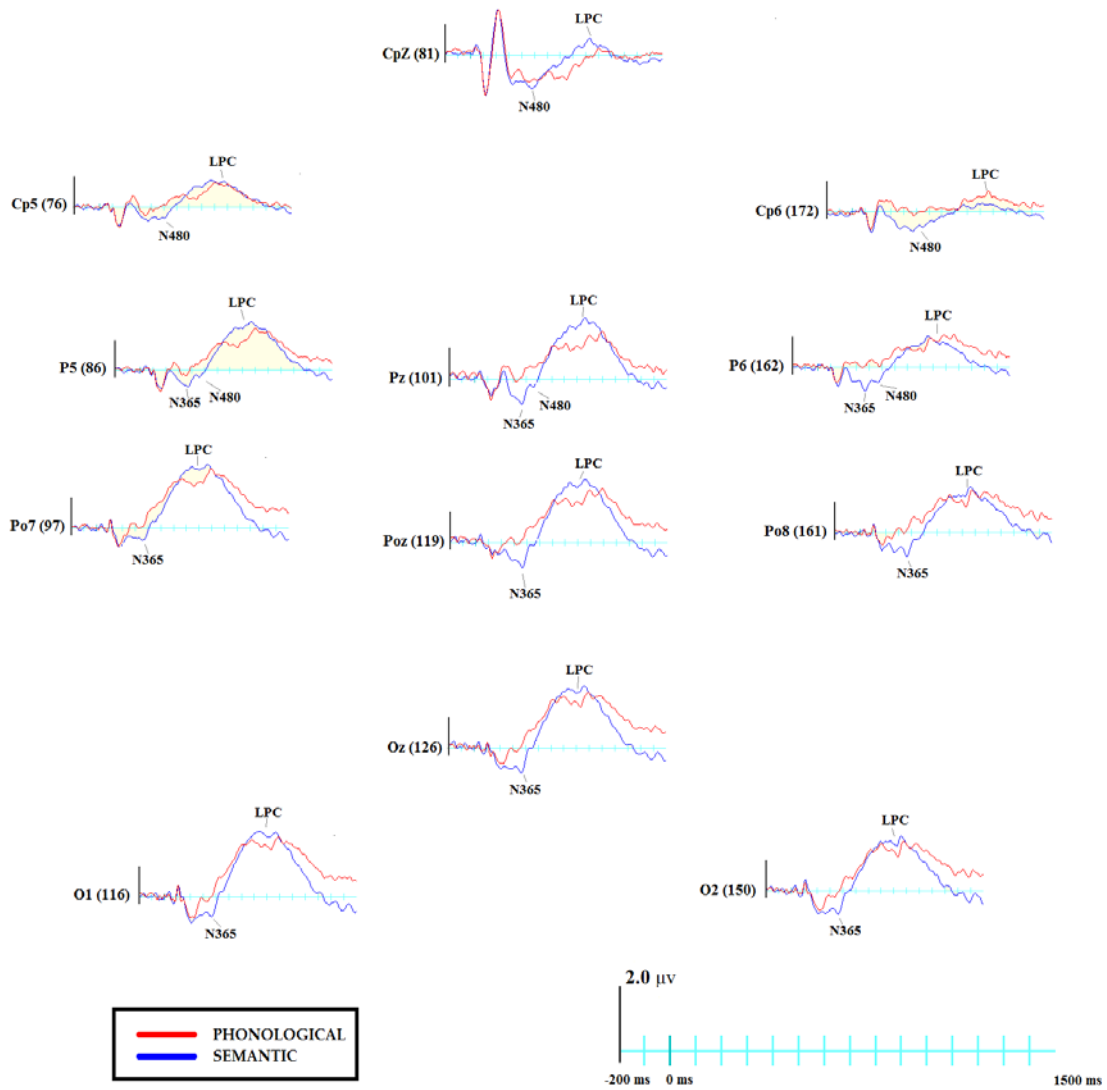


*Figure 7.* ERPs at Posterior Scalp Locations. The N365, N480, and LPC can be seen for the phonological condition (in red) and the semantic condition (in blue).

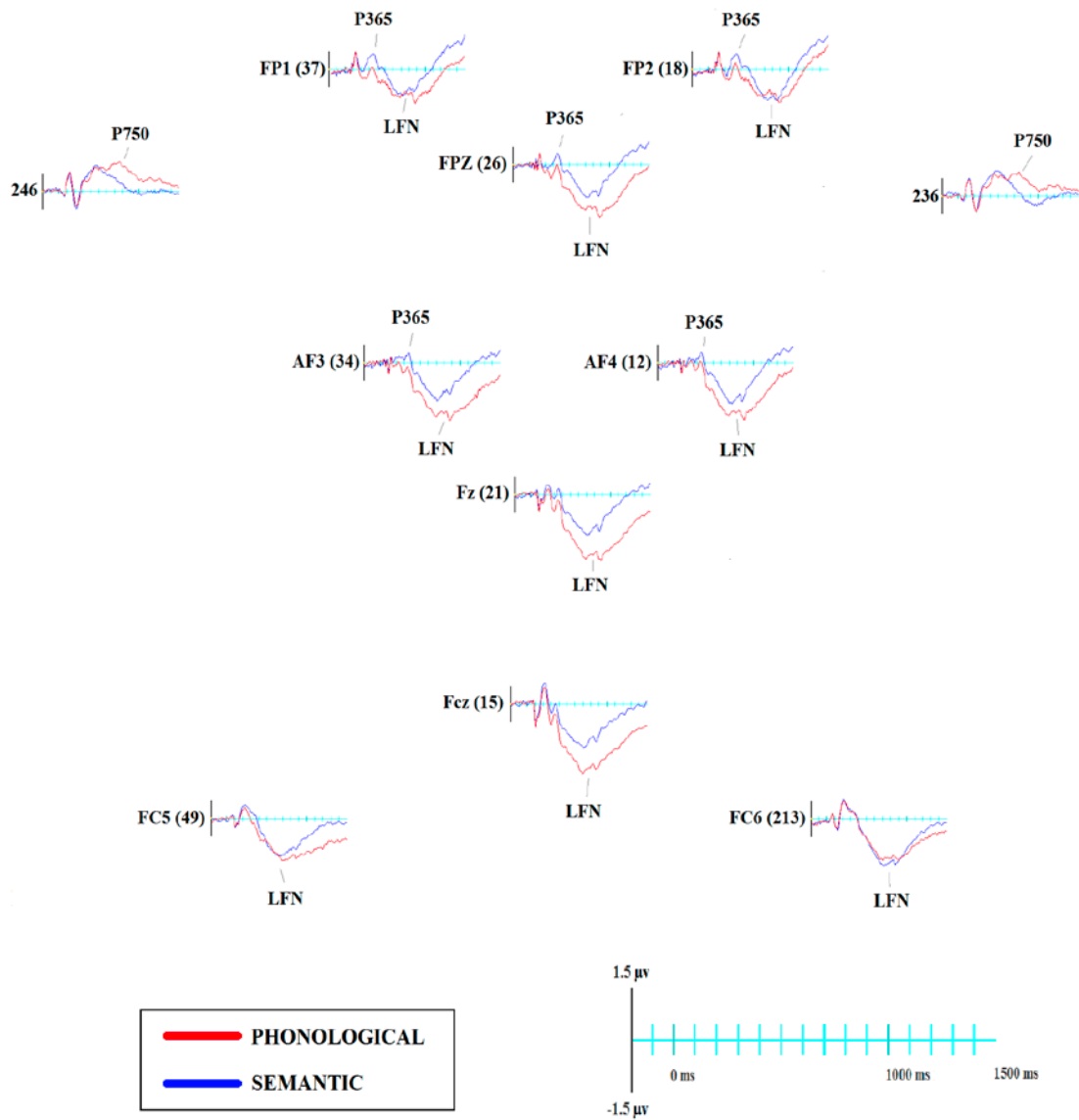


Figure 8. ERPs at Anterior Scalp Locations. The P365, LFN, and the LAVP can be seen for the phonological condition (in red) and the semantic condition (in blue).

## Source Localization

### Source waveforms

Source waveforms were output for regions of interests and other highly active locations for both the phonological and semantic conditions. Source analysis was carried out on the grand average of each of these conditions. The source waveforms can be seen in figure 9.

### N400-window components

#### *N365/P365*

The N365/P365 for both phonological and semantic conditions localized strongest to bilateral medial temporal lobes (BA 35, BA 36, BA 38, and hippocampal gyri), and bilateral ventromedial prefrontal cortex (BA 11, BA 25, amygdala gyri), respectively. The semantic condition showed a higher intensity of source localized activity than the phonological condition at medial temporal and ventromedial prefrontal regions. The N365 for the semantic condition also localized to more posterior areas, BA 30, BA 31, and BA 37 which were not seen for the phonological condition. Overall, activations for both the phonological and semantic conditions were slightly more intense in the left hemisphere. Full flat maps and an MRI slice view at the peak of the N365 component can be seen in figure 10.

#### *N480*

The N480 showed a very similar pattern of source localized activity as the N365, namely the strong medial temporal sources, which was stronger for the semantic condition.



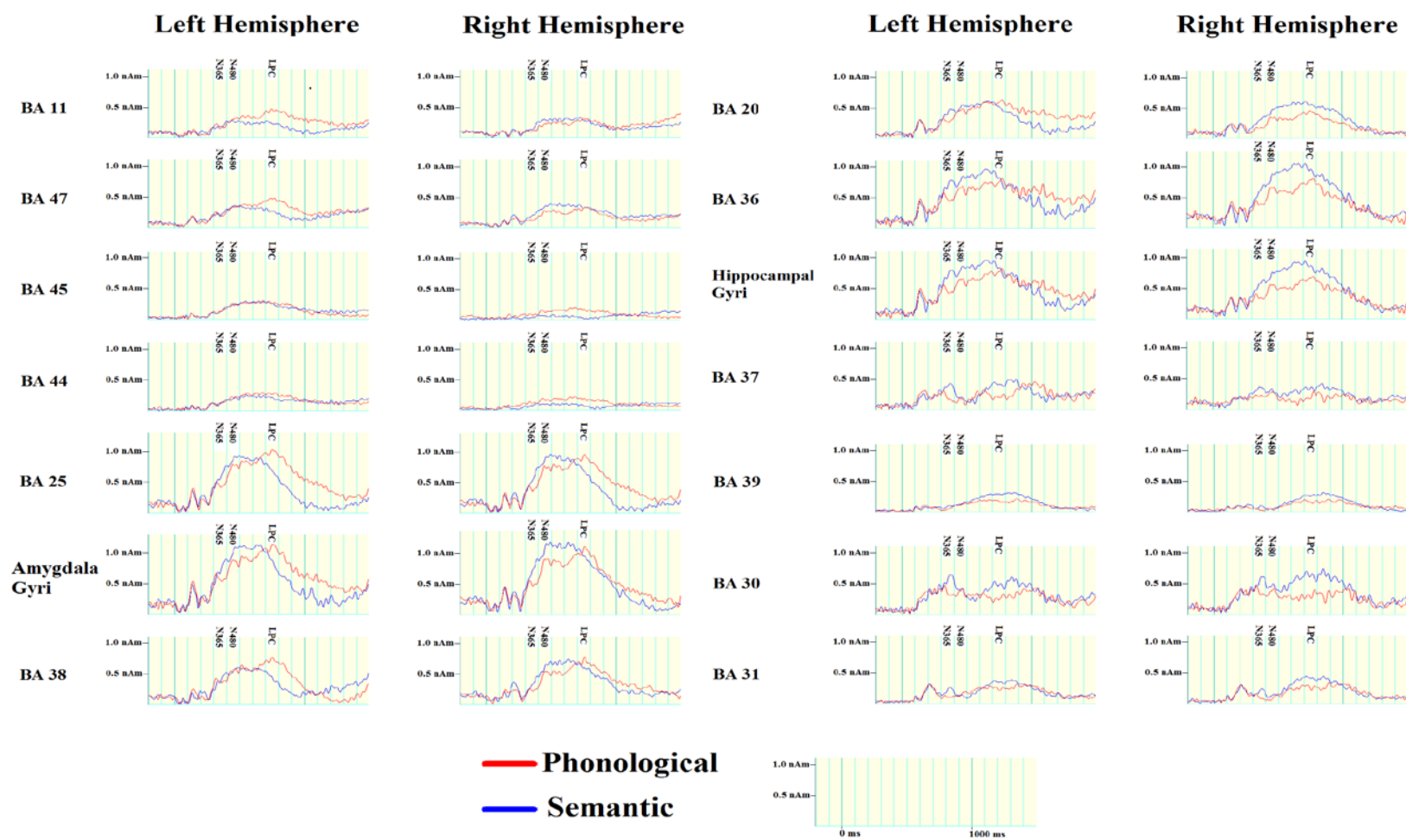
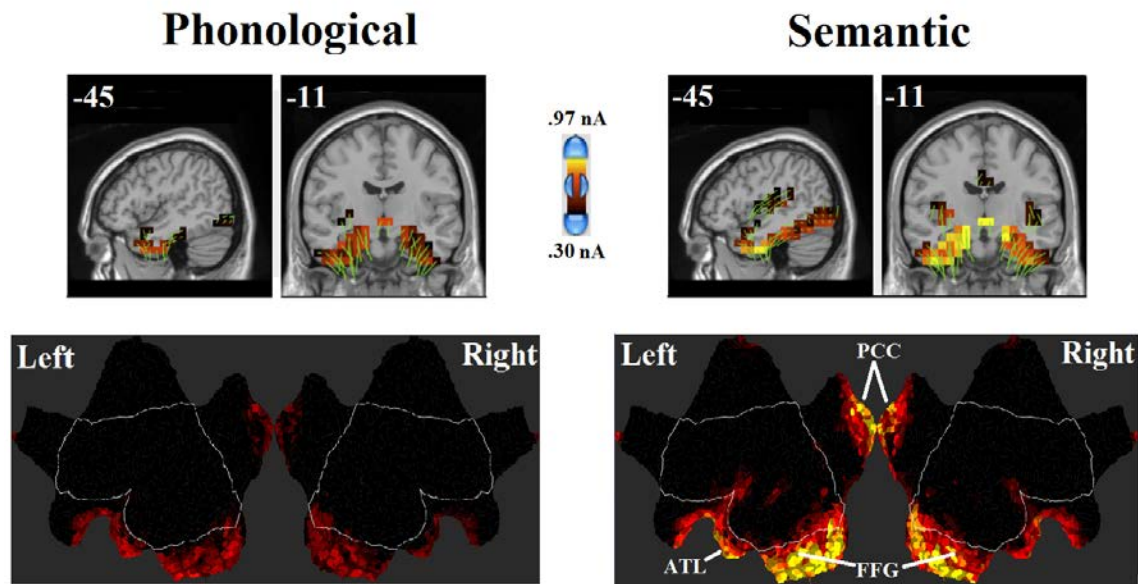


Figure 9. Source waveforms. The source waveforms are plotted from -200 to 1500 ms. Brodmann areas and other regions with high source localized activity were included.

The N480 was larger for the semantic condition, and again both phonological and semantic conditions showed a slight left hemisphere bias. Posterior activity, however, dropped off sharply between the offset of the N365 and the onset of the N480. Full flat maps and an MRI slice view at the peak of the N480 component can be seen in figure 11.



*Figure 10.* Source Solution at 365 ms (Approximate Peak of the N365) for phonological and semantic grand average ERPs. Sagittal, coronal, and flat map images are shown for each condition. The number in the top left corner of the MRI slice view images represent the MNI x and y coordinates. The scale in the middle of the MRI slice view images indicates the strength of source localized activity in nano amp/meters.

## Late components

### *LPC 650 ms*

The LPC started at about 650 ms and strongly localized bilaterally to anterior medial temporal regions (BA 20, BA28, BA34, BA 35, and BA 36) for both phonological

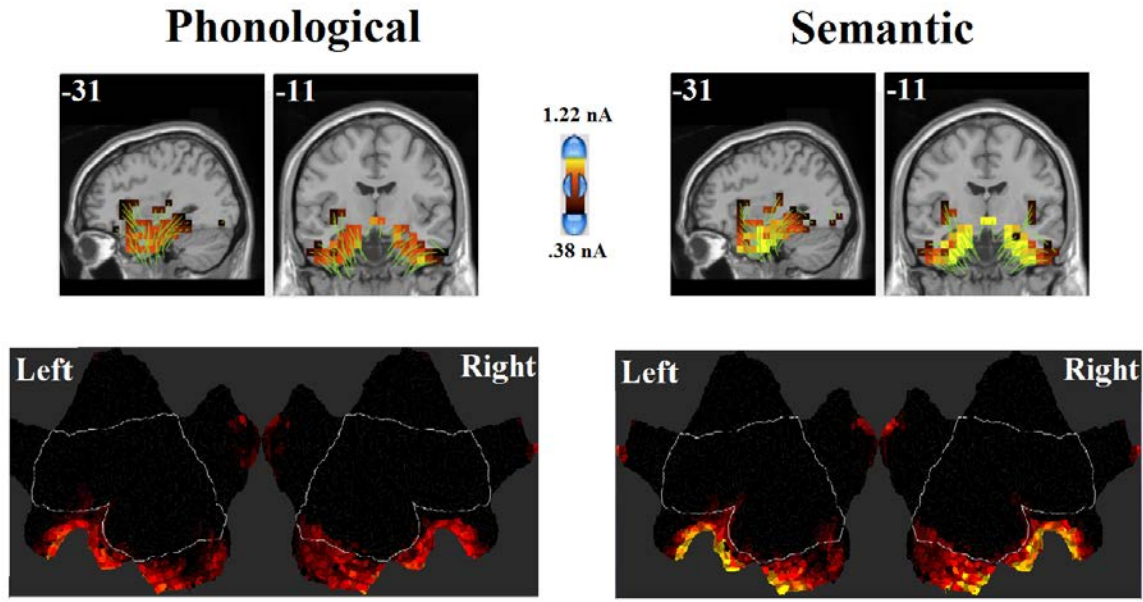


*Figure 11.* Source Solution at 480 ms (Approximate Peak of the N480) for phonological and semantic grand average ERPs. Sagittal, coronal, and flat map images are shown for each condition. The number in the top left corner of the MRI slice view images represent the MNI x and y coordinates. The scale in the middle of the MRI slice view images indicates the strength of source localized activity in nano amp/meters.

and semantic conditions, but activity in ventromedial prefrontal cortices (BA 11 and BA 25) was also seen at this time point for both conditions. This activity was largest in the left hemisphere for the phonological condition. Frontal activations were more pronounced in the phonological condition. The semantic condition was also showing activity in bilateral posterior cingulate cortex. Activations for both phonological and semantic conditions were slightly left lateralized. Both semantic and phonological conditions showed activity in superior temporal and insula regions of the left hemisphere that were not present in the right hemisphere. Posterior cingulate and angular gyrus were beginning to show more activity for the semantic condition at this time point, which was not seen for the phonological condition. Full flat maps and an MRI slice view at 650 ms can be seen in figure 12.

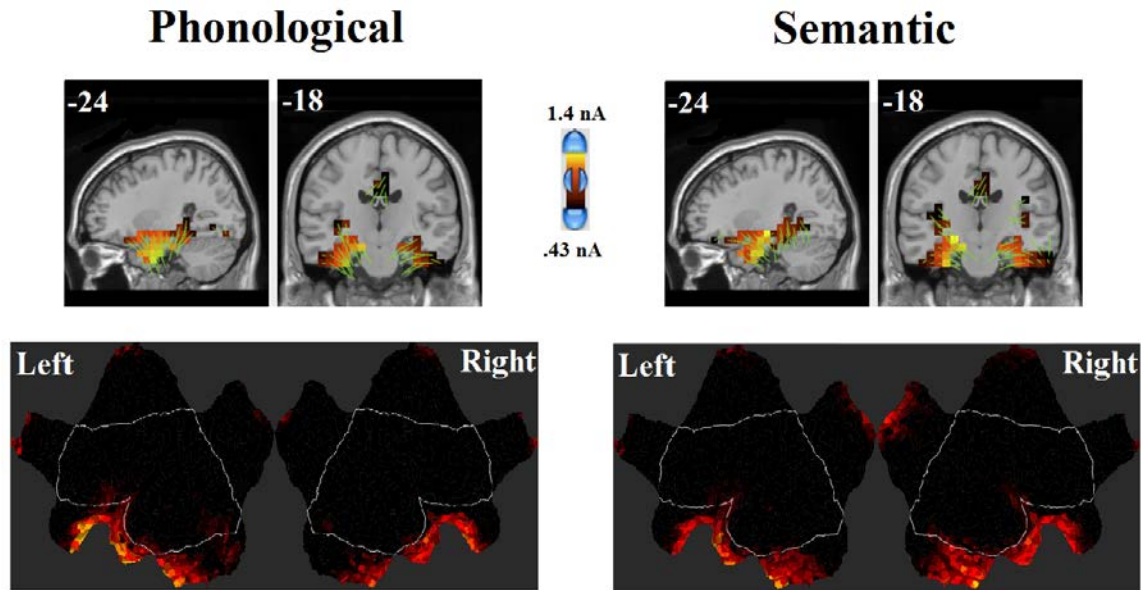


*Figure 12.* Source Solution at 650 ms (Approximate Start of the LPC) for phonological and semantic grand average ERPs. Sagittal, coronal, and flat map images are shown for each condition. The number in the top left corner of the MRI slice view images represent the MNI x and y coordinates. The scale in the middle of the MRI slice view images indicates the strength of source localized activity in nano amp/meters.

### ***LAVP***

At the approximate peak of the LAVP at 750 ms, there was an increase in frontal polar activity; this was especially strong for the phonological condition. Both conditions were still showing high activity in bilateral medial temporal lobes and ventromedial prefrontal cortices. Overall, source localized activity for the phonological condition was strongest at frontal regions, while again the semantic condition had more posterior activations in bilateral temporal and parietal lobes. Full flat maps and an MRI slice view at the peak of the LAVP component can be seen in figure 13.

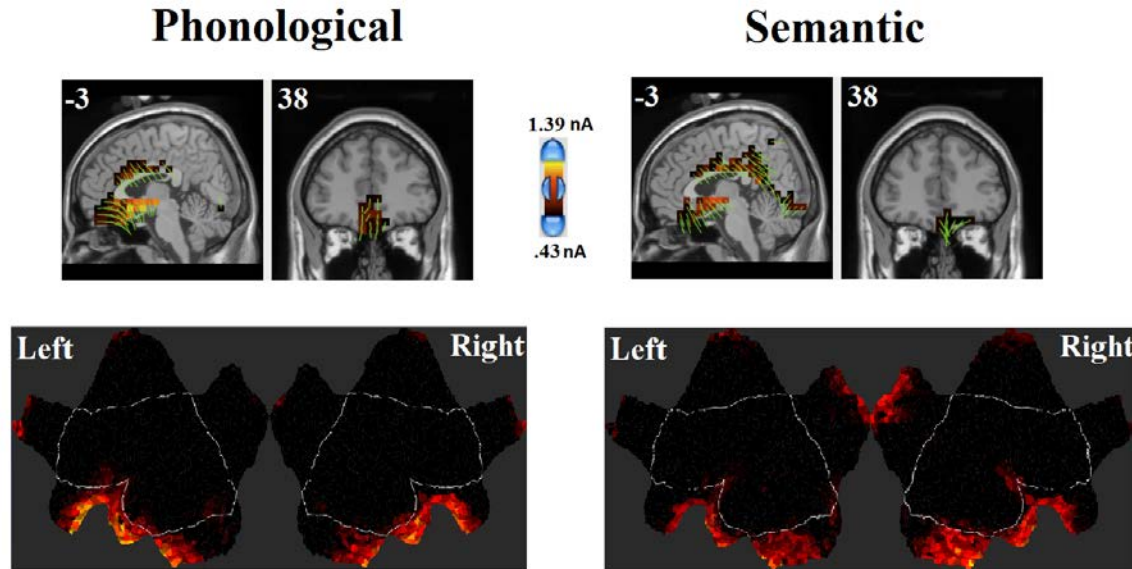


*Figure 13.* Source Solution at 750 ms (Approximate Peak of the LAVP) for phonological and semantic grand average ERPs. Sagittal, coronal, and flat map images are shown for each condition. The number in the top left corner of the MRI slice view images represent the MNI x and y coordinates. The scale in the middle of the MRI slice view images indicates the strength of source localized activity in nano amp/meters.

### ***LPC 850 ms***

It was at time point, 850 ms, when the differences in LPC amplitude for the semantic and phonological conditions were the greatest. Notably, there was a large difference in source localized activity between the two conditions. The phonological condition showed more ventromedial prefrontal activity (BA 11, BA 25, and BA 38), lateral prefrontal (BA 47), and temporal pole (BA 38) activity, whereas the semantic condition showed much more posterior cingulate, angular gyrus, and fusiform gyrus activity (BA 30, BA 31, BA 39, BA 37). Full flat maps and an MRI slice view at 850 ms can be seen in figure 14.

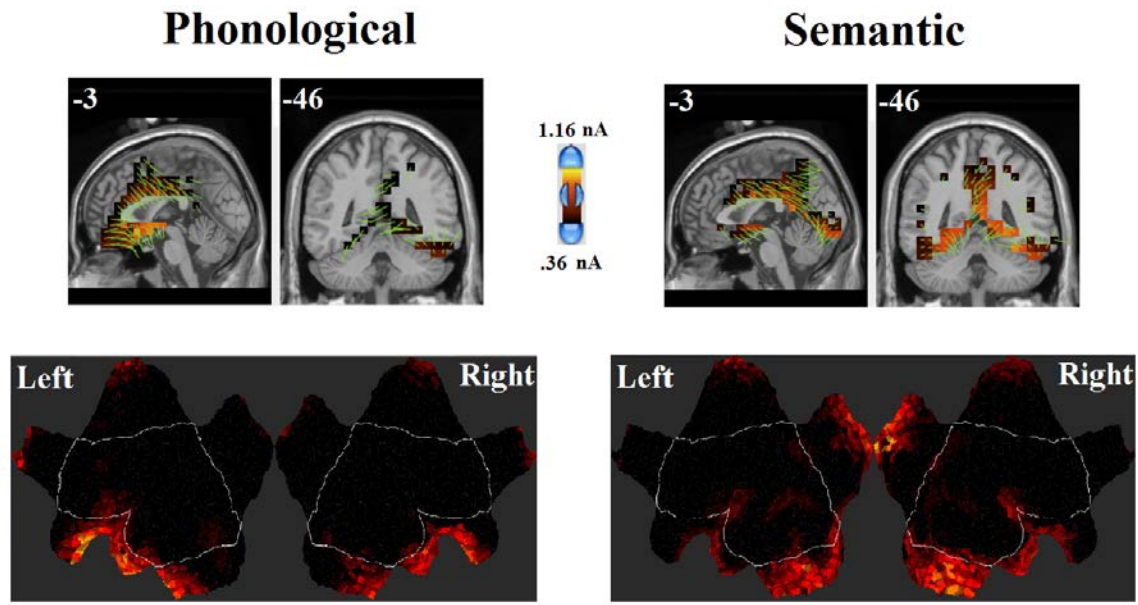


Figure 14. Source Solution at 850 ms (Approximate Peak of the LPC) for phonological and semantic grand average ERPs. Sagittal, coronal, and flat map images are shown for each condition. The number in the top left corner of the MRI slice view images represent the MNI x and y coordinates. The scale in the middle of the MRI slice view images indicates the strength of source localized activity in nano amp/meters.

### Difference wave source analysis vs. fMRI subtraction

We conducted Student's t-tests subtracting the phonological condition from the semantic condition in an attempt to isolate semantic-specific processing (see figure 15 for t-test topographic maps from 50 to 900 ms). This t-wave, or simply a difference wave, is often used to illustrate the N400 effect, in which stimuli that are more semantically difficult to integrate elicit a larger N400. In an attempt to isolate the semantic system we then compared the source localization of the t-wave to the Binder et al. (2008) fMRI results from their semantic – phoneme task contrasts, from which our tasks were adapted. The GeoSource MRI slice views were thresholded to display the top 60% of source localized activity (see Figure 16). Later components were not explored in this manner

because topography of the waveforms for each condition began to differ too much; that is, at some scalp locations the electrical potentials were larger for the phonological condition, and at other locations the electrical potentials were larger for the semantic condition. This appears to be due to a variety of different components contributing to the LPC and later potentials which are difficult to interpret. A comparison of the t-test wave source estimates vs. the Binder et al. (2008) fMRI bold activations can also be seen in figure 16.

## CHAPTER IV

### DISCUSSION

The aim of this study was to evaluate the ability of EEG source localization to localize the complex cognitive process of semantics in language. This study had the advantage of being very similar to an fMRI study (Binder et al., 2008). This allowed for additional means of interpreting the source solutions, in addition to current semantic and language models.

#### **Early Components**

Because the P1-N1-P2 complex is thought to be a response to processing of sound properties, it makes sense that the topographies for the phonological and semantic conditions would be very similar, because they are either word or word-like speech sounds carefully controlled and recorded by the same speaker. Although attempts were made to control the tone stimuli in a similar fashion, their inherent simple acoustic structures were considerably different than the speech sounds of the other two conditions. This simplistic acoustic structure, particularly its sharper and highly consistent onset, is likely to have been the cause of the much larger N1 seen for the acoustic condition (Coch, Sanders, & Neville, 2005; Hillyard et al., 1973; Sanders, Stevens, Coch, & Neville, 2006).



## N400-Window Components

### Scalp

There seemed to be two distinct N400-like components with slightly different topographies, but both are in the typical centroparietal region and time window for the N400. It is not uncommon for the N400 to be measured at multiple times and labeled as N400a, N400b, and N400c (e.g. Perrin & Garcia-Larrea, 2003) as the negativity can often span several hundred milliseconds. However, in this case there were two distinct negative peaks for the semantic condition, (N364 and N480) and only one for the phonological condition (N364). The N400 is thought to index lexical semantic access to stored representations. Because participants were asked to actively interpret the words they heard in a meaningful context, it required participants to effortfully analyze each word in terms of its meaning and respond appropriately. Although, the CV triplets were word-like, participants were asked to focus on the phonology of the CV triplet, rather than trying to make meaning of the CV triplet. Thus, the increased semantic processing required in the semantic condition is reflected by the increase in amplitude of both N400-like components.

The two N400-like components in this study look similar to what was found by other researchers using a very similar semantic task in which participants were asked to press yes if the word they heard was a clothing item, and no if it was not (Mehta, Jerger, Jerger, & Marin, 2009). Their ICA analysis revealed separate components for these two distinct negativities. The first negativity was interpreted as phonological processing and the second as semantic processing. This idea is consistent with the analysis of acoustic

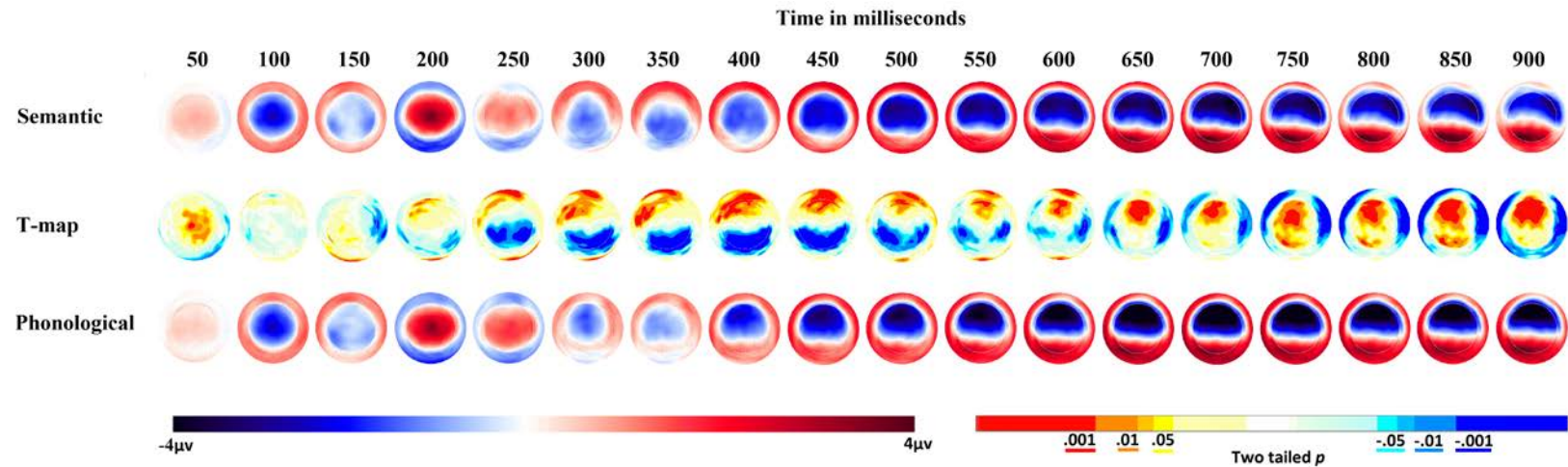


*Figure 15.* Topographic Maps of the Semantic – the Phonological Condition from 50 ms to 900 ms. In the topo-maps for the semantic and phonological conditions, blue indicates negative electrical potentials and red indicates positive electrical potentials, which range from  $-4 \mu\text{V}$  to  $4 \mu\text{V}$ . The t-test topo map is displaying the t values of the student's t-test (red colors representing positive t values and blue colors representing negative t values). The corresponding  $p$  values range from 0 to .001 with alpha set at .05.

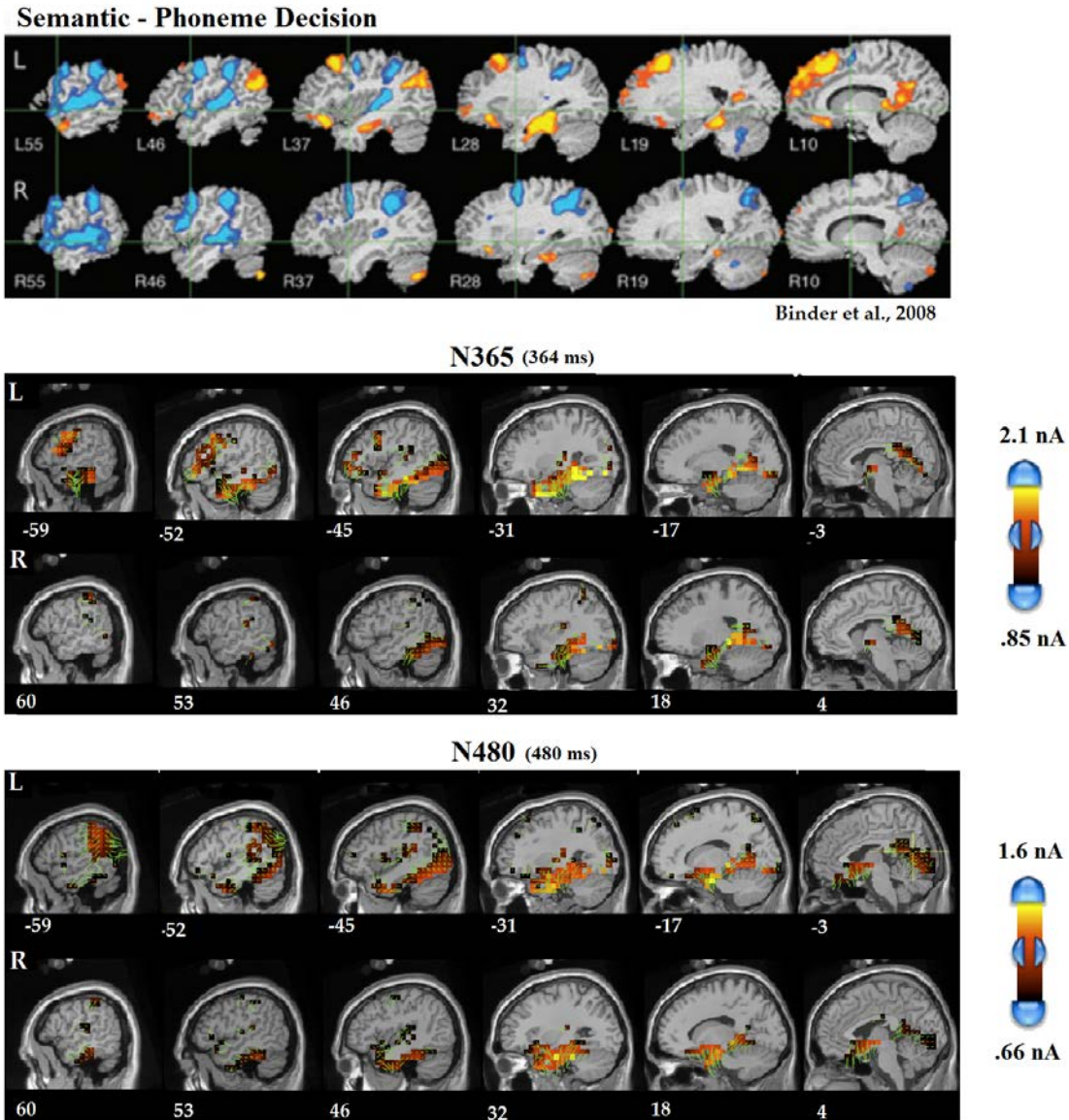


*Figure 16.* MRI View Comparison with the Binder et al. (2008) Semantic - Phoneme Decision Tasks. The top figure is from the Binder et al. (2008) study using nearly identical experimental tasks and contrast. The bottom two images are the source localizations of the t-test wave (semantic - phonological) at N365 and N480.

and phonological characteristics of auditory stimuli taking place before semantic recognition (Price, 2010), and further supported by the difference in the phonological and semantic conditions of this study. There are two distinct negativities seen for the semantic condition, and only one distinct negativity seen for the phonological condition.

## **N400-window source localization**

The source localization of the N365 grand average was consistent with past EEG source localization research, indicating inferior temporal, inferior occipital, anterior temporal, medial temporal and posterior cingulate/angular gyrus current sources (Silva-Pereyra et al., 2003; Frishkoff et al., 2004). This was especially true for the semantic condition, which implicated several strong current sources in these regions. However, the phonological condition implicated far fewer current sources that survived thresholding, but did have fairly strong localization to left anterior temporal lobe. Source localization with MEG studies suggest a strong source, the N400, coming from the middle temporal gyrus, especially in the left hemisphere. (Dale et al., 2000; Maess, Herrmann, Hahne, Nakamura, & Friederici, 2006).

The N480 in the current study also source localized very strongly to bilateral medial temporal lobes and much of inferior temporal and occipital lobes, as well as anterior temporal lobe. Nevertheless, the N480 did not show strong source localization to the posterior cingulate gyrus. This suggests at least some unique source information can be gleaned from both of the N400-like components and that the two components may represent different processes.

The middle temporal and inferior temporal regions have been suggested as a store of lexical representations that are accessed by other parts of the semantic network (Hickok & Poeppel, 2007; Lau & Poeppel, 2008). A review of language 100 fMRI studies shows that word stimuli typically activate more inferior temporal and posterior brain regions (Price, 2010). The posterior cingulate and anterior temporal lobes are important areas in the semantic network. Their function is thought to integrate incoming

information into current contextual and syntactic representations (Hickok & Poeppel, 2007; Lau & Poeppel, 2008). Damage to posterior, middle and superior temporal regions have been associated with comprehension deficits (Bates et al., 2003; Boatman, 2004; Goodglass, 1993). Consistent with the involvement of these regions in the semantic network, they showed a higher intensity of source localized activity for the semantic condition than the phonological condition.

### **Later Components**

#### **LPC – consistent with P3b**

It is very common for typical N400 paradigms to elicit a late positivity, often called “LPC” or “P300.” The P3b is a subcomponent of the P3 or LPC, which is maximal over parietal scalp. The P3b is evoked during stimulus processing and is believed to index brain activity related to context-updating and subsequent memory storage (Polich, 2007). In this study the phonological condition showed a smaller P3b. The phonological task requires participants to quickly evaluate each of the three consonant-vowel pairs. Binder and colleagues (2008) concluded the phonological task placed higher demands on phonological working memory. Although P3 amplitude is sometimes found to be larger with increased task demands, it is also often found to be smaller as a result of increased memory and perceptual load (see Kok, 2001 for a review). In the present study, the smaller LPC associated with the phonological condition, and larger LPC with the semantic condition is likely due to at least two factors. First, the increase in perceptual load associated with three separate consonant-vowel pairs is likely to have led to an overlap in P3a and various subcomponents of the P3b, which are shifted in time and therefore not adding together like they might in a simpler condition (Kok, 2001), such as

the semantic task. The shift could also be in part due to some of the CV triplet stimulus sets being more difficult than others, which would cause a later LPC for the more difficult trials. Second, in the semantic condition, participants are drawing more on long term memory stores as they evaluate each word. Stimuli with particular meaning or salience or invoking memory retrieval have been found to increase P3 amplitudes (Kok, 2001; Polich, 2007). An examination of the topography of the LPC across phonological and semantic conditions, show there are multiple subcomponents of the LPC, which appear to sum in the semantic condition at approximately 850 ms, while there appears to be a more complex series of late components for the phonological condition that do not sum together.

### **Late component source localization**

The start of the LPC (approximately 650 ms post stimulus onset) localized to much of the medial temporal lobes and more strongly to anterior temporal regions. Overall, the sources at the start of the LPC were very similar to what was seen for the N365 and N480. The most noticeable difference was the left lateralization of current sources for the phonological condition, whereas the semantic condition showed more bilateral current sources. Even at the peak of the LPC, at approximately 850 ms, the phonological condition showed left lateralized current source estimates, and the semantic condition was to a great extent bilateral. Nevertheless, at this point there are many more prefrontal, frontal, and anterior temporal current source estimates for the phonological condition, and many more posterior and inferior parietal current source estimates for the semantic condition. Anterior cingulate and prefrontal current sources seen for the phonological condition were consistent with the increase in attention and phonological

working memory required for the phonological task. The anterior temporal lobe has been implicated as a region involved in mapping phonological representations onto lexical conceptual representations (Hickok & Poeppel, 2007). This may also be reflected by the increased anterior temporal activity for the phonological condition. Electrical activity for the semantic condition was localized strongly to angular gyrus and posterior cingulate cortex, as well as inferior and medial temporal regions (fusiform gyrus, parahippocampal and hippocampal cortex). The angular gyrus (sometimes referred to as the temporal-parietal junction) is important in the semantic network and thought to be involved in concept retrieval and conceptual integration (Binder, Desai, Graves, & Conant, 2009; Lau et al., 2008). This activity was likely reflecting increased semantic analysis and constraints in context of the semantic decision task.

## **LAVP**

The LAVP peaked at 750 ms and thus overlapped with the LPC. The LAVP was only seen for the phonological condition. The LAVP localized strongly to frontal pole, anterior cingulate, inferior frontal, medial frontal, subcallosal gyrus, and medial temporal lobes. The semantic condition showed more posterior sources in temporal, parietal, and cingulate regions, but also showed less intense frontal polar and anterior cingulate activity. These frontal regions together make up the ventral medial prefrontal cortex, which have been implicated in working memory, response conflict, error detection, and executive control functions (Binder et al., 2009). It seems likely this time period reflected cognitive resource allocation required for both conditions, and the extra attentional and working memory demands associated with the phonological task.

## Semantic – Phoneme T-test Wave

The t-test maps revealed the phonological and semantic condition were quite similar, until approximately 250 ms post stimulus. The N400-like components were also examined using this difference wave. Unlike the source analysis of the individual average conditions, source analysis of the t-test wave should ideally highlight features that differ between the two conditions. The t-test wave at the peak of the N365 also localized most strongly to bilateral inferior and anterior temporal lobes, though with a much stronger left hemisphere bias. This is exactly what would be expected for an ERP indexing semantic processing. Furthermore, orbitofrontal, ventrolateral, and dorsolateral frontal regions showed high estimates of current sources, which were present exclusively in the left hemisphere. There was only mild source localization to posterior cingulate cortex, and no localization to angular gyrus at the time of the N365. However, at the time of the N480, there was strong localization to angular gyrus, supramarginal gyrus, and posterior cingulate. This activity was also strongly left lateralized. Medial temporal sources evenly localized to both left and right hemispheres at the time of the N480. Frontal source estimates seen for the N365 correspond well with our knowledge of the inferior frontal gyrus in language as being involved in retrieval and selection of lexical representations (Lau et al., 2008; Price, 2010).

This strong left lateralization for both N400-like components seen for the t-test wave was not seen for the individual condition grand averages of the phonological or semantic conditions, though there were some slight hemisphere biases. Furthermore, the t-test wave localized to many more frontal structures than would be expected (Frishkoff et al., 2004; Lau et al., 2008; Silva-Pereyra et al., 2003). This suggests that contrasting



the conditions with at the scalp with a t-wave before source analysis may be more effective at accurately characterizing intrahemispheric source generators.

### **Limitations**

The non-invasive nature of EEG, and its advantages is apparent. However, language mapping using dense array EEG source localization needs to be further validated against established fMRI and DCS paradigms to better assess its effectiveness at localizing language. More accurate source localization could also be achieved by using an individual head model, instead of the generic head model in this study. Ultimately if dense array EEG is to be used as a clinical tool for mapping language, source analysis should be conducted on individual subject ERPs, rather than a grand average. Better source modeling of language is thus likely to be achieved with individual ERPs and head models. For the present study, source localization of a grand average using a generic head model seemed appropriate and a logical and necessary first step. Results of the t-test wave source localization at the N400-window components were consistent with the Binder et al., 2008 semantic – phoneme contrast in localizing strong left lateralized sources, particularly with respect to medial temporal, frontopolar, posterior cingulate, and angular gyrus sources. EEG source analysis localized more inferior temporal and more lateral frontal regions. I think overall the dense array EEG source analysis in the present study was fairly consistent with the Binder et al., 2008 fMRI findings with respect to the t-test wave source localization results, but not very consistent with respect to individual condition grand averages ERP source localization results.

## **Conclusions**

Overall, the present paradigm, which was adapted and modified from a well-designed fMRI study that was 100% concordant with the Wada test, appeared to be well suited for an EEG study. EEG source localization was successful in highlighting several important cortical brain regions involved in language processing. The t-test wave appeared to do a better job of localizing frontal regions, and more accurately characterizing the dominant hemisphere for language than did localization of the individual language condition grand averages separately.

APPENDIX A

EDINBURGH HANDEDNESS INVENTORY

Please indicate with a check (✓) your preference in using your left or right hand in the following tasks.

Where the preference is so strong you would never use the other hand, unless absolutely forced to, put two checks (✓✓).

If you are indifferent, put one check in each column (✓ | ✓).

Some of the activities require both hands. In these cases, the part of the task or object for which hand preference is wanted is indicated in parentheses.

Task / Object	Left Hand	Right Hand
1. Writing		
2. Drawing		
3. Throwing		
4. Scissors		
5. Toothbrush		
6. Knife (without fork)		
7. Spoon		
8. Broom (upper hand)		
9. Striking a Match (match)		
10. Opening a Box (lid)		
Total checks:	LH =	RH =
Cumulative Total	CT = LH + RH =	
Difference	D = RH - LH =	
Result	R = (D / CT) <input type="checkbox"/>	
Interpretation: (Left Handed: R < -40) (Ambidextrous: -40 <input type="checkbox"/> (Right Handed: R > +40)		

APPENDIX B

BLOCK DESIGN COUNTERBALANCING

<u>Set 1:</u>	<u>Set 2:</u>	<u>Set 3:</u>	<u>Set 4:</u>	<u>Set 5:</u>	<u>Set 6:</u>
Tone 1	Tone 1	Phoneme 1	Phoneme 1	Semantic 1	Semantic 1
Phoneme 1	Semantic 1	Tone 1	Semantic 1	Tone 1	Phoneme 1
Semantic 1	Phoneme 1	Semantic 1	Tone 1	Phoneme 1	Tone 1
Tone 2	Tone 2	Phoneme 2	Phoneme 2	Semantic 2	Semantic 2
Phoneme 2	Semantic 2	Tone 2	Semantic 2	Tone 2	Phoneme 2
Semantic 2	Phoneme 2	Semantic 2	Tone 2	Phoneme 2	Tone 2
Tone 3	Tone 3	Phoneme 3	Phoneme 3	Semantic 3	Semantic 3
Phoneme 3	Semantic 3	Tone 3	Semantic 3	Tone 3	Phoneme 3
Semantic 3	Phoneme 3	Semantic 3	Tone 3	Phoneme 3	Tone 3
Tone 4	Tone 4	Phoneme 4	Phoneme 4	Semantic 4	Semantic 4
Phoneme 4	Semantic 4	Tone 4	Semantic 4	Tone 4	Phoneme 4
Semantic 4	Phoneme 4	Semantic 4	Tone 4	Phoneme 4	Tone 4

**36 Trials / Block**

**144 total stimuli / Condition**

APPENDIX C

SEMANTIC CONDITION STIMULUS LIST

ANIMALS	PLANTS	OCCUPATIONS	FOODS
<b>butterfly</b>	<b>blackberry</b>	<b>architect</b>	<b>alfredo</b>
<b>dragonfly</b>	<b>blueberry</b>	<b>attorney</b>	<b>cannoli</b>
<b>honeybee</b>	<b>cantaloupe</b>	<b>botanist</b>	<b>gelato</b>
<b>ladybug</b>	<b>cranberry</b>	<b>coroner</b>	<b>lasagna</b>
<b>mockingbird</b>	<b>honeydew</b>	<b>pharmacist</b>	<b>panini</b>
<b>mosquito</b>	<b>mandarin</b>	<b>physicist</b>	<b>parmesan</b>
<b>nightingale</b>	<b>raspberry</b>	<b>professor</b>	<b>provolone</b>
<b>pelican</b>	<b>strawberry</b>	<b>scientist</b>	<b>ricotta</b>
<b>woodpecker</b>	<b>tomato</b>	<b>therapist</b>	<b>spumoni</b>
anteater	apricot	accountant	anchovy
antelope	banana	astronaut	baklava
barnacle	broccoli	auditor	biscotti
buffalo	carnation	barista	bologna
chinchilla	celery	bartender	bruschetta
centipede	coconut	carpenter	burrito
chimpanzee	cucumber	conductor	caviar
cockatoo	daffodil	consultant	cereal
coyote	hickory	counselor	chocolate
crocodile	juniper	designer	escargot
elephant	lavender	detective	fajita
flamingo	nectarine	director	granola
gorilla	papaya	engineer	hamburger
caribou	peppermint	fisherman	havarti
halibut	persimmon	gardener	jellybean
iguana	pimento	hypnotist	licorice
jellyfish	pineapple	journalist	linguine
kangaroo	poinsettia	mechanic	marmalade
manatee	potato	minister	pastrami
parakeet	rosemary	mortician	potsticker
piranha	sesame	musician	salami
platypus	sunflower	novelist	spaghetti
porcupine	tangerine	pianist	tamale
rattlesnake	violet	programmer	tempura
scorpion	wasabi	reporter	tortilla
Wallaby	watercress	stonemason	tostada
wolverine	zucchini	surveyor	venison

*Note.* Target stimuli for each category are in bold font.

APPENDIX D

PHONOLOGICAL CONDITION STIMULUS LIST

TARGETS	STANDARDS		
kupæto	bæjapu	fapodo	pæsælu
siputæ	rirupi	kapimi	polusa
hæpætæ	fafopu	hæpivæ	pubæma
japutu	naræpa	yapiga	pomolæ
dæpata	vuvapo	dupægi	pobiro
rapato	fizopu	mupudi	pisælæ
wutapo	hizipi	niparæ	pænanu
votæpa	jodæpa	hapugæ	pilisu
fætipo	rimopa	supano	poloræ
motæpæ	buhupu	hipuræ	pogobu
gatipu	hulapæ	fupadu	puræda
butæpu	zafipa	fupalo	pijano
pitano	suhæpa	mipuræ	parira
pitira	sogopa	bipidi	pamolu
pitaru	sunapi	rupæbo	padivu
pitæga	molipu	læpæhu	pihælæ
pætasa	gufipa	dopiho	pugoma
pætiru	nimæpæ	sopænu	pæmælu
pæbutu	læsita	botoru	tæfæna
pomætu	dubito	fætækæ	tunili
pozito	dofita	gotari	takori
pafatæ	kokota	fitæku	tobavi
pijitæ	mækuto	jitædo	tædila
pomito	gonota	ratowo	tozæfi
tupibæ	ginæta	wotomi	tomaru
tupulo	kælatæ	nitora	tufosa
topinæ	sisotæ	wutugæ	tinæmæ
tipava	dærity	futubæ	togaho
tapihu	gimoto	lutyi	tagima
topodo	yabæta	gætohæ	tæbugu
towopu	jirotu	jutilæ	tamamo
tomipæ	sonutu	hætæba	tonuki
tukipi	hodota	litæfu	tonanæ
tadupa	sukata	bitila	tamoji
tulapo	lunæta	hætaro	tænihu
tifæpi	fumita	jutusæ	tæliju

## APPENDIX E

### ACCOUSTIC CONDITION STIMULUS LIST

<b>600Hz-500Hz-600Hz</b>	800Hz-700Hz-600Hz
600Hz-500Hz-700Hz	<b>800Hz-700Hz-800Hz</b>
600Hz-700Hz-500Hz	800Hz-700Hz-900Hz
600Hz-700Hz-600Hz	800Hz-900Hz-700Hz
600Hz-700Hz-800Hz	800Hz-900Hz-800Hz
600Hz-800Hz-600Hz	800Hz-900Hz-1000Hz
600Hz-800Hz-700Hz	800Hz-1000Hz-800Hz
700Hz-500Hz-600Hz	900Hz-700Hz-800Hz
<b>700Hz-500Hz-700Hz</b>	<b>900Hz-700Hz-900Hz</b>
700Hz-600Hz-500Hz	900Hz-800Hz-700Hz
<b>700Hz-600Hz-700Hz</b>	<b>900Hz-800Hz-900Hz</b>
700Hz-600Hz-800Hz	900Hz-800Hz-1000Hz
700Hz-800Hz-600Hz	900Hz-1000Hz-800Hz
700Hz-800Hz-700Hz	900Hz-1000Hz-900Hz
700Hz-800Hz-900Hz	1000Hz-800Hz-900Hz
700Hz-900Hz-700Hz	<b>1000Hz-800Hz-1000Hz</b>
800Hz-600Hz-700Hz	1000Hz-900Hz-800Hz
<b>800Hz-600Hz-800Hz</b>	<b>1000Hz-900Hz-1000Hz</b>

*Note.* Target tone trains are in bold font.

## REFERENCES CITED

- Bates, E., Wilson, S. M., Saygin, A. P., Dick, F., Sereno, M. I., Knight, R. T., & Dronkers, N. F. (2003). Voxel-based lesion-symptom mapping. [Comparative Study Research Support, U.S. Gov't, Non-P.H.S. Research Support, U.S. Gov't, P.H.S.]. *Nature Neuroscience*, 6(5), 448-450. doi: 10.1038/nm1050
- Bizzi, A., Blasi, V., Falini, A., Ferroli, P., Cadioli, M., Danesi, U., . . . Broggi, G. (2008). Presurgical functional MR imaging of language and motor functions: validation with intraoperative electrocortical mapping. [Validation Studies]. *Radiology*, 248(2), 579-589. doi: 10.1148/radiol.2482071214
- Binder, J. R., Desai, R. H., Graves, W. W., & Conant, L. L. (2009). Where is the semantic system? A critical review and meta-analysis of 120 functional neuroimaging studies. [Meta-Analysis Research Support, N.I.H., Extramural Review]. *Cerebral Cortex*, 19(12), 2767-2796. doi: 10.1093/cercor/bhp055
- Binder, J. R., Frost, J. A., Hammeke, T. A., Bellgowan, P. S., Rao, S. M., & Cox, R. W. (1999). Conceptual processing during the conscious resting state. A functional MRI study. [Research Support, Non-U.S. Gov't Research Support, U.S. Gov't, P.H.S.]. *Journal Cognitive Neuroscience*, 11(1), 80-95.
- Binder, J. R., Rao, S. M., Hammeke, T. A., Frost, J. A., Bandettini, P. A., Jesmanowicz, A., & Hyde, J. S. (1995). Lateralized human brain language systems demonstrated by task subtraction functional magnetic resonance imaging. [Research Support, Non-U.S. Gov't Research Support, U.S. Gov't, P.H.S.]. *Archives of Neurology*, 52(6), 593-601.
- Binder, J. R., Swanson, S. J., Hammeke, T. A., Morris, G. L., Mueller, W. M., Fischer, M., . . . Houghton, V. M. (1996). Determination of language dominance using functional MRI: a comparison with the Wada test. [Comparative Study Research Support, Non-U.S. Gov't]. *Neurology*, 46(4), 978-984.
- Binder, J. R., Swanson, S. J., Hammeke, T. A., & Sabsevitz, D. S. (2008). A comparison of five fMRI protocols for mapping speech comprehension systems. *Epilepsia*, 49(12), 1980-1997. doi: EPI1683 [pii]10.1111/j.1528-1167.2008.01683.x
- Baxendale, S. (2009). The Wada test. *Current Opinion in Neurology*, 22(2), 185-189. doi: 10.1097/WCO.0b013e328328f32e
- Boatman, D. (2004). Cortical bases of speech perception: evidence from functional lesion studies. *Cognition*, 92, 47-65.
- Bookheimer, S. (2007). Pre-surgical language mapping with functional magnetic resonance imaging. *Neuropsychology Rev* 17(2): 145-155.



- Coch, D., Sanders, L.D., & Neville, H. (2005). An event related potential study of selective auditory attention in children and adults. *Journal of Cognitive Neuroscience*, 17, 605-622.
- Dale, A. M., Liu, A. K., Fischl, B. R., Buckner, R. L., Belliveau, J. W., Lewine, J. D., & Halgren, E. (2000). Dynamic statistical parametric mapping: combining fMRI and MEG for high-resolution imaging of cortical activity. [Research Support, Non-U.S. Gov't; Research Support, U.S. Gov't, Non-P.H.S.; Research Support, U.S. Gov't, P.H.S.]. *Neuron*, 26(1), 55-67.
- Giussani, C., Roux, F. E., Ojemann, J., Sganzerla, E. P., Pirillo, D., & Papagno, C. (2010). Is preoperative functional magnetic resonance imaging reliable for language areas mapping in brain tumor surgery? Review of language functional magnetic resonance imaging and direct cortical stimulation correlation studies. *Neurosurgery*, 66(1), 113-120. doi: 10.1227/01.NEU.0000360392.15450.C9
- Goodglass, H. (1993). Understanding Aphasia (pp. 210-211). San Diego, CA: Academic Press.
- Halgren, E., Dhond, R. P., Christensen, N., Van Petten, C., Marinkovic, K., Lewine, J. D., & Dale, A. M. (2002). N400-like magnetoencephalography responses modulated by semantic context, word frequency, and lexical class in sentences. *Neuroimage*, 17, 1101-1116.
- Helenius, P., Salmelin, R., Service, E., & Connolly, J. F. (1998). Distinct time courses of word and context comprehension in the left temporal cortex. *Brain*, 121, 1133-1142.
- Hickok, G., & Poeppel, D. (2007). The cortical organization of speech processing. [Research Support, N.I.H., Extramural Review]. *Nature Reviews Neuroscience*, 8(5), 393-402. doi: 10.1038/nrn2113
- Hillyard, S. A., Hink, R.F., Schwent, V.L., & Picton, T.W. (1973). Electrical signs of selective attention in the human brain. *Science*, 182(4108), 177-180.
- Holmes, M. D., Tucker, D. M., Quiring, J. M., Hakimian, S., Miller, J. W., & Ojemann, J. G. (2010). Comparing noninvasive dense array and intracranial electroencephalography for localization of seizures. [Comparative Study]. *Neurosurgery*, 66(2), 354-362. doi: 10.1227/01.NEU.0000363721.06177.07
- Holmes, C. J., Hoge, R., Collins, L., Woods, R., Toga, A. W., & Evans, A. C. (1998). Enhancement of MR images using registration for signal averaging. [Comparative Study; Research Support, Non-U.S. Gov't; Research Support, U.S. Gov't, Non-P.H.S.; Research Support, U.S. Gov't, P.H.S.]. *Journal of Computer Assisted Tomography*, 22(2), 324-333.

- Junghofer, M., Elbert, T., Tucker, D. M., & Braun, C. (1999). The polar average reference effect: a bias in estimating the head surface integral in EEG recording. [Research Support, Non-U.S. Gov't]. *Clinical Neurophysiology*, 110(6), 1149-1155.
- Frishkoff, G. A., Tucker, D. M., Davey, C., & Scherg, M. (2004). Frontal and posterior sources of event-related potentials in semantic comprehension. [Research Support, U.S. Gov't, P.H.S.]. *Brain Research. Cognitive Brain Research*, 20(3), 329-354. doi: 10.1016/j.cogbrainres.2004.02.009
- Kok, A. (2001). On the utility of P3 amplitude as a measure of processing capacity. [Review]. *Psychophysiology*, 38(3), 557-577.
- Kutas M & Federmeier, K.D. (2009), *Scholarpedia*, 4(10):7790. doi:10.4249/scholarpedia.7790, revision #91545
- Lau, E. F., Phillips, C., & Poeppel, D. (2008). A cortical network for semantics: (de)constructing the N400. [Research Support, N.I.H., Extramural Research Support, U.S. Gov't, Non-P.H.S.]. *Nature Reviews. Neuroscience*, 9(12), 920-933. doi: 10.1038/nrn2532
- Lurito, J. T., Lowe, M. J., Sartorius, C., & Mathews, V. P. (2000). Comparison of fMRI and intraoperative direct cortical stimulation in localization of receptive language areas. [Comparative Study]. *Journal of Computer Assisted Tomography*, 24(1), 99-105.
- Michel, C. M., Murray, M. M., Lantz, G., Gonzalez, S., Spinelli, L., & Grave de Peralta, R. (2004). EEG source imaging. *Clinical Neurophysiology*, 115, 2195-2222.
- Maess, B., Herrmann, C. S., Hahne, A., Nakamura, A., & Friederici, A. D. (2006). Localizing the distributed language network responsible for the N400 measured by MEG during auditory sentence processing. [Research Support, Non-U.S. Gov't]. *Brain Research*, 1096(1), 163-172. doi: 10.1016/j.brainres.2006.04.037
- Ojemann, G., Ojemann, J., Lettich, E., & Berger, M. (1989). Cortical language localization in left, dominant hemisphere. An electrical stimulation mapping investigation in 117 patients. [Research Support, U.S. Gov't, P.H.S.]. *Journal of Neurosurgery*, 71(3), 316-326. doi: 10.3171/jns.1989.71.3.0316
- Oldfield, R. C. (1971). The assessment and analysis of handedness: The Edinburgh inventory. *Neuropsychologia*, 9, 97-113.
- Pascual-Marqui, R. D. (2002). Standardized low-resolution brain electromagnetic tomography (sLORETA): technical details. *Methods and Findings in Experimental and Clinical Pharmacology*, 24 Suppl D, 5-12.

- Perrin, F., & Garcia-Larrea, L. (2003). Modulation of the N400 potential during auditory phonological/semantic interaction. [Research Support, Non-U.S. Gov't]. *Brain Research. Cognitive Brain Research*, 17(1), 36-47.
- Perrin, F., Pernier, J., Bertrand, O., Giard, M., & Echallier, J. F. (1987). Mapping of scalp potentials by surface spline interpolation. *Electroencephalography and Clinical Neurophysiology*, 66, 75-81.
- Polich, J. (2007). Updating P300: an integrative theory of P3a and P3b. [Research Support, N.I.H., Extramural Review]. *Clinical Neurophysiology*, 118(10), 2128-2148. doi: 10.1016/j.clinph.2007.04.019
- Price, C. J. (2010). The anatomy of language: a review of 100 fMRI studies published in 2009. *Ann New York Academy of Sciences*, 1191, 62-88. doi: NYAS5444 [pii] 10.1111/j.1749-6632.2010.05444.x
- Pulgram, E. (1970). Syllable, word, nexus, cursus. The Hague: Mouton, 131 p. 23
- Roux, F. E., Boulanouar, K., Lotterie, J. A., Mejdoubi, M., LeSage, J. P., & Berry, I. (2003). Language functional magnetic resonance imaging in preoperative assessment of language areas: correlation with direct cortical stimulation. [Evaluation Studies]. *Neurosurgery*, 52(6), 1335-1345; discussion 1345-1337.
- Sanders, L.D., Stevens, C., Coch, D. & Neville, H.J. (2006). Selective auditory attention in 3- 5-year-old children: an event-related potential study. *Neuropsychologia* 44, 2126–2138.
- Spreer, J., Arnold, S., Quiske, A., Wohlfarth, R., Ziyeh, S., Altenmuller, D., . . . Schumacher, M. (2002). Determination of hemisphere dominance for language: comparison of frontal and temporal fMRI activation with intracarotid amytal testing. [Comparative Study Evaluation Studies]. *Neuroradiology*, 44(6), 467-474. doi: 10.1007/s00234-002-0782-2
- Swanson, S. J., Sabsevitz, D. S., Hammeke, T. A., & Binder, J. R. (2007). Functional magnetic resonance imaging of language in epilepsy. *Neuropsychology Rev*, 17(4), 491-504. doi: 10.1007/s11065-007-9050-x
- Titone, D., & Connine M. (1987). Syllabification strategies in spoken word processing: Evidence from phonological priming. *Psychology Research*, 60, 251-263.
- Tomczak, R. J., Wunderlich, A. P., Wang, Y., Braun, V., Antoniadis, G., Gorich, J., . . . Brambs, H. J. (2000). fMRI for preoperative neurosurgical mapping of motor cortex and language in a clinical setting. *Journal of Computer Assisted Tomography*, 24(6), 927-934.

- Tse, C.-Y., Lee, C.-L., Sullivan, J., Garnsey, S.M., Dell, G.S., Fabiani, M., & Gratton, G. (2007). Imaging cortical dynamics of language processing with the event-related optical signal. *Proceedings of the National Academy of Sciences of the United States of America*, 104(43), 17157-17162.
- Silva-Pereyra, J., Rivera-Gaxiola, M., Aubert, E., Bosch, J., Galan, L., & Salazar, A. (2003). N400 during lexical decision tasks: a current source localization study. [Research Support, Non-U.S. Gov't]. *Clinical Neurophysiology*, 114(12), 2469-2486.
- Wada, J. (1949). A new method for determination of the side of cerebral speech dominance: A preliminary report on the intracarotid injection of sodium amytal in man. *Igaku Seibutsugaku*, 4, 221-222
- Worthington, C., Vincent, D. J., Bryant, A. E., Roberts, D. R., Vera, C. L., Ross, D. A., & George, M. S. (1997). Comparison of functional magnetic resonance imaging for language localization and intracarotid speech amytal testing in presurgical evaluation for intractable epilepsy. Preliminary results. [Comparative Study]. *Stereotactic and Functional Neurosurgery*, 69(1-4 Pt 2), 197-201.
- Yetkin, F. Z., Mueller, W. M., Morris, G. L., McAuliffe, T. L., Ulmer, J. L., Cox, R. W., . . . Haughton, V. M. (1997). Functional MR activation correlated with intraoperative cortical mapping. *American Journal of Neuroradiology*, 18(7), 1311-1315.